A Non-Linear Market Model*

Tobias Sichert

Department of Finance

Stockholm School of Economics

tobias.sichert@hhs.se

December 5, 2023

Abstract

I show that non-linear pricing of market risk can explain many prominent cross-sectional stock return anomalies, such as momentum, betting-against-beta, idiosyncratic volatility, and liquidity. The non-linear pricing model is inferred from options data without assumptions on the pricing relationship. I further document that many anomalies have a strong tail risk exposure, which is successfully priced by the model. A key feature of the model is a sizable upside risk premium of approximately 4% per annum. Finally, the pricing results can be explained with a compensation for exposure to systematic variance risk.

JEL classification: G10, G12, G13

Keywords: Pricing kernel, anomalies, upside risk, variance risk, risk premia, skewness, tail risk

*I thank Caio Almeida, Daniel Andrei, Magnus Dahlquist, Adrien d'Avernas, Bob Dittmar, Mathieu Fournier (discussant), Stefano Giglio, Amit Goyal, Cam Harvey, Michael Hasler, Burton Hollifield, Jan Pieter Krahnen, Lars-Alexander Kühn, Lasse Pedersen, Simon Rottke, Riccardo Sabbatucci, Christian Schlag, Maik Schmeling, David Schreindorfer, Zhaneta Tancheva (discussant), Julian Thimme, Christian Wagner, Rüdiger Weber, Irina Zviadadze (discussant); conference participants of the DGF, JEF, NFA, SED; and seminar participants at the universities of Arizona State, Carnegie Mellon, Collegio Carlo Alberto, Göteborg, Goethe, Nova SBE, Princeton, Stockholm School of Economics, Toronto, Zürich, and Warwick for valuable comments and suggestions. Some of the results herein appeared in an earlier version of this paper under the title "The Pricing Kernel Is U-shaped".

I. Introduction

Although the linear capital asset pricing model (CAPM) is clearly one of the most popular models of modern financial economics, abundant empirical evidence suggests that it is misspecified. These findings have spurred the search for alternative sources of systematic risk. One obvious approach is to consider a non-linear pricing model, but doing so requires finding ways to discipline the potentially infinite number of non-linear pricing functions. A common approach is to assume a representative agent and derive the non-linearity implied by the agent's marginal utility function. Prominent examples include coskewness risk (Harvey and Siddique 2000), cokurtosis risk (Dittmar 2002), and downside risk (Ang et al. 2006a, among others). However, these parametric approaches often cannot explain many of the existing return anomalies. Moreover, standard utility functions rule out non-monotonic pricing functions, which, in turn, have empirical support from the options data (Jackwerth 2000; Aït-Sahalia and Lo 2000; Rosenberg and Engle 2002).

In this paper, I suggest an alternative approach to obtain a non-linear market model without imposing any structure on the pricing relationship. I rely on the S&P 500 options market, where non-linear payoffs are traded and priced. Specifically, I use standard tools from the literature to estimate the option-implied pricing kernel. This pricing kernel determines the pricing of market risk and reveals how investors' marginal utility varies with returns. My paper is the first to use this pricing kernel to study the cross-sectional patterns in expected stock returns.

The empirical results show that the non-linear pricing of market risk inferred from option prices can correctly price a large set of prominent stock return anomalies, both in US and European data. In particular, these anomalies include sorts based on CAPM-beta, volatility, idiosyncratic volatility, momentum, turnover, zero-trade, sensitivity to aggregate volatility, past maximum return, and industry, which all have large alphas relative to the CAPM. The pricing kernel that I suggest and which makes all these alphas vanish is a function of only the market return. Its functional form is estimated fully out-of-sample using only index options and index return data. Moreover, it uses no cross-sectional return information or factor-mimicking portfolios, and is therefore not estimated to fit the cross-section.

A well-known property of the estimated option-implied pricing kernel is its non-monotonic U-shape (Bakshi et al. 2010; Christoffersen et al. 2013; Song and Xiu 2016), which is illustrated

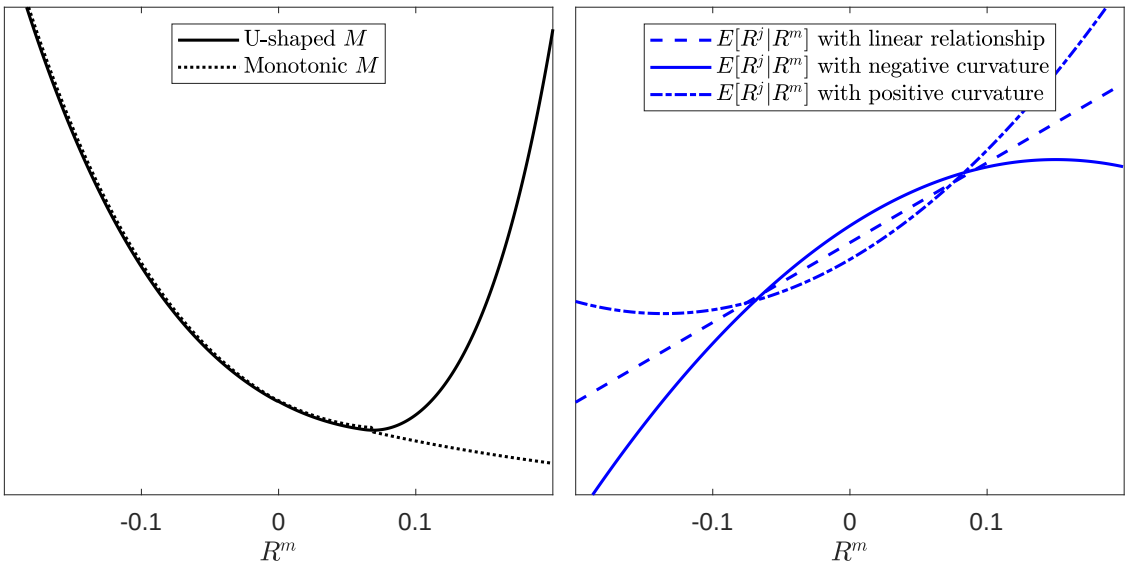

Figure 1: **Stylized pricing kernels and return relationships with curvature.** The left graph illustrates a stylized U-shaped pricing kernel M together with a monotonic M. The right graph illustrates the returns R^j of asset j that have either a linear relationship, or positive and negative return curvature relative to the market return R^m.

in the left graph of Figure 1. Of importance for this study, the U-shaped pricing kernel is increasing in the area of positive returns, which implies an upside risk premium. I show that this upside risk premium, which is absent in existing factor models, explains on average half of the alphas of both the CAPM and the Fama and French (1993) three-factor model, and up to 89% in case of the low beta anomaly. Furthermore, across aforementioned anomalies, upside risk is on average associated with a statistically significant risk premium of 4.0% per annum. The prevalence and magnitude of the upside risk premium is strikingly consistent across a variety of asset classes. In particular, when using this kernel to price several options and commodity portfolios, I again find a significant upside risk premium of about 50% of the CAPM alpha. Finally, applying the analogous approach to European equities portfolios delivers results very similar to those for the US and thus confirms the US results out-of-sample.

To put the results into perspective, the analysis starts with the derivation of two theoretical properties of the data-generating process that are necessary for non-linear pricing of risk to outperform linear pricing. These two conditions are, first, a systematic non-linear dependence between the market returns and anomaly returns, and second, that this dependence must be inversely related to the pricing kernel.

Next, I test these conditions in the data. Starting with the first condition, I document a striking feature of many prominent anomalies that I refer to as "curvature patterns." The returns of portfolios with positive CAPM alphas exhibit a negative curvature relative to the market return, and vice versa. As can be seen in the right graph of Figure 1, portfolios with negative curvature significantly underperform the linear relationship, both in times of large positive and large negative market returns. In other words, many anomalies have a strong, systematic risk exposure on both tails of the market return distribution.

Schneider et al. (2020) document this pattern for the low beta and the idiosyncratic volatility anomalies. I show that this pattern is much more widespread by studying all 95 portfolio sorts considered in Gu et al. (2020) using my 1996–2019 sample. I find that when the sorting variable is based on market data (stock returns or trading volume), the portfolio sorts tend to have strong curvature patterns. A total of 16 sorts fall into this category and include all aforementioned anomalies, and in addition various other measures of momentum, volatility and stock liquidity, as well as industry sorts. In contrast, portfolio sorts based on accounting data variables do not display such patterns.

I next examine the second condition. The risk premium (i.e., the expected excess return) R^j on any asset j can be written as

$$E\left[R^j\right] = -\text{Cov}\left[R^j, M\right] \times R_f. \tag{1}$$

All else equal, a more negative curvature implies that the portfolio returns are more negatively correlated with a U-shaped pricing kernel M and, therefore, require a higher risk premium. Focusing on the upside, the negative curvature, together with the U-shaped M, induces an additional upside risk premium. Portfolios with a positive curvature, in contrast, are more positively correlated with a U-shaped M and, therefore, are hedge assets in both tails and earn low returns on average.

While numerous studies show that downside risk is priced in the cross-section of stock returns (e.g., Ang et al. 2006a; Kelly and Jiang 2014; Lettau et al. 2014; Farago and Tédongap 2018), upside risk has received much less attention in the literature. Although a few papers have extended their stock-level downside risk measure to an upside risk measure, they generally find weak and insignificant upside risk premia at the individual stock level (Ang et al. 2006a;

Chabi-Yo et al. 2018). In contrast, I find that the upside risk is significantly priced at the portfolio level. This divergence is related to my finding that many well-know portfolios have strong and persistent curvature patterns and hence tail risk exposure, while stock-level measures of tail exposure have low persistence (e.g., Ang et al. 2006a; Barahona et al. 2021).

To interpret my pricing results economically, I link them to an explanation based on variance risk. The finding of a non-monotonic option-implied pricing kernel is often referred to as the "pricing kernel puzzle," since it is at odds with the monotonicity predicted by many classical theories. A promising explanation for this puzzle is variance risk, as suggested by Chabi-Yo (2012), Christoffersen et al. (2013), and Bakshi et al. (2022). This explanation is appealing for at least two reasons: first, because the variance risk premium is empirically well-documented and, second, because the enormous trading volumes in options and other volatility-related derivatives show that investors are clearly concerned about variance risk.

However, from the perspective of existing equilibrium models, the U-shaped pricing kernel is still a puzzle, as it is unclear whether these relationships from reduced-form models can also be obtained in a structural model. To close the gap between theoretical models and the empirical evidence and illustrate the link, I show that a modified Bansal and Yaron (2004) long-run risks model can generate a U-shaped pricing kernel, by introducing GARCH-type dynamics for the variance of consumption growth, which measures uncertainty of economic fundamentals. The key feature of these dynamics is that they exhibit a feedback mechanism in which consumption shocks impact future variance, leading to an increase in economic uncertainty following both large positive and large negative consumption shocks.[1] I provide supporting evidence for this property in consumption data. As dividends are modeled as levered consumption, the new feature connects large positive market returns with increases in uncertainty on average. Due to her Epstein and Zin (1989) preferences, the representative agent dislikes high uncertainty about future consumption growth, and hence these states of the world are associated with high marginal utility. In other words, a high positive market return is indicative of an increase in uncertainty about economic fundamentals, which the agent dislikes more than the large positive consumption growth associated with it.

Building on these arguments, I empirically test whether my pricing results are consistent

[1] Tédongap (2015) also studies a long-run risks model with GARCH dynamics but does not study the projected pricing kernel or upside risk.

with investors being compensated for their exposure to systematic variance. Specifically, I use the returns to a variance contract (i.e., the asset that costs VIX^2 and pays the monthly realized variance) as an additional pricing factor. This extended and U-shaped market model again delivers low and insignificant pricing errors, which shows that exposure to systematic variance can indeed explain the otherwise anomalous portfolio returns. In other words, referring back to the curvature patterns from Figure 1, many anomalies exhibit a payoff profile that resembles a short straddle, and — just like the options position — they earn positive excess returns relative to the CAPM in compensation for losses in both tails. As extreme returns in both tails tend to coincide with spikes in realized variance, a variance-averse investor dislikes these states of the world and therefore requires an additional risk premium for portfolios with negative curvature.[2] Thus, while the extant literature proposes many alternative explanations for *individual* anomalies — too many to cite here — this paper provides a unified *joint* explanation for several prominent anomalies.

This explanation differs from those of existing studies on the pricing of market variance risk in equities in two important ways. First, based on an ICAPM argument, several studies show that shocks to future expected variance are priced in the cross-section (Ang et al. 2006b; Bansal et al. 2014; Campbell et al. 2018). In contrast, I show that using realized variance as an additional factor can explain numerous return anomalies. Second, I document that realized variance has a U-shaped relationship to the contemporaneous index return; hence, the model generates a U-shaped pricing kernel. In contrast, shocks to future expected variance have a monotonically decreasing relationship with the index return and therefore do not generate upside risk.

The explanation based on variance risk suggested in this paper is related to the coskewness model of Kraus and Litzenberger (1976) and Harvey and Siddique (2000). In a more recent empirical test, Schneider et al. (2020) show that the model can explain the low beta and the idiosyncratic volatility anomaly. I differ from these studies in several ways. First, my pricing model can explain a substantially larger number of stock return anomalies as well as the expected returns of other asset classes, most of which the coskewness factor fails to explain. Second, my

[2]The findings further suggest that the pricing of risks in the options and stock markets are consistent and that the two markets are integrated. This conclusion is in contrast to several papers that argue that the two markets are partially segmented (e.g., Bollen and Whaley 2004; Garleanu et al. 2008; Dew-Becker and Giglio 2022; Frazzini and Pedersen 2022).

approach allows me to study the effect of upside and downside risk separately, whereas most existing approaches cannot differentiate between the two. In fact, while the coskewness literature usually emphasizes downside risk, I highlight that upside risk is substantial and relevant for understanding anomaly returns. Third and related, I provide an economic explanation for upside risk via variance risk. In contrast, in the coskewness model, upside risk only emerges as a technical artifact from a second-order Taylor series expansion of the utility function.[3] Fourth, my approach does not rely on a factor-mimicking portfolio to measure the market price of risk, instead obtaining it directly from the options data.

The remainder of the paper proceeds as follows. Section II studies the non-linear pricing of market risk theoretically and provides empirical evidence for curvature patterns in returns. Section III introduces the estimation methodology for the pricing kernel, along with the estimation results. The pricing results and their robustness are presented in Section IV. Section V shows that a variance risk-based explanation can empirically reconcile the results. Section VI outlines an equilibrium framework that generates an upside risk premium, and Section VII concludes. The appendix provides technical details, and the internet appendix contains derivations, additional results, and robustness checks.

[3]Several theories that depart from rational expectation also imply qualitatively that stocks with positive return skewness have low returns, on average. Examples include the endogenous optimal beliefs model of Brunnermeier et al. (2007), the heterogeneous skewness preference model of Mitton and Vorkink (2007), and the cumulative prospect theory model of Barberis and Huang (2008). In contrast to these theories, I provide a quantitative explanation based on variance risk. In addition, I focus on systematic risk at the portfolio level, while the aforementioned theories focus on idiosyncratic skewness at the stock level, which quickly diversifies away when aggregating stocks into portfolios.

II. Non-linear Pricing and Curvature Patterns in Asset Returns

This section discusses the theoretical conditions under which non-linear pricing of risk matters. I then verify the first condition in the data, namely, that asset returns have a systematic, non-linear relationship relative to the index returns. I begin by presenting a detailed empirical example using the idiosyncratic volatility anomaly, and then generalize this finding to many equity portfolios and other asset classes. The second condition is verified in the estimation and pricing results in Sections III – V.

A. Conditions required for non-linear pricing to matter

Let $M_{t+1} = M_t(R^m_{t+1})$ denote a pricing kernel that is a potentially non-linear function of the market excess return R^m such that the Euler equation

$$E_t[M_{t+1}R^m_{t+1}] = 0 \tag{2}$$

holds. In principle, the pricing kernel can be a function of many sources of risk; hence, $M(R^m)$ denotes only the pricing kernel projected onto R^m. As discussed in Cochrane (2005), the projected pricing kernel has the same pricing implications as the original kernel for all assets which payoffs depend only on R^m. The conditions under which it prices any other asset's excess return R^j depends on the structure of the economy.

To address this question, one can formally ask whether

$$E_t[M_{t+1}R^j_{t+1}] = 0 \tag{3}$$

also holds. To proceed, I have to make further assumptions on the data-generating process. To intuit the relevance of non-linear pricing, consider the following setup:

$$R^j_{t+1} = \beta^j R^m_{t+1} + \epsilon_{t+1}, \tag{4}$$

and three potential assumptions on the CAPM pricing errors ϵ:

$$\text{Case 1: } E_t[\epsilon_{t+1}|R^m_{t+1}] = 0, \tag{5}$$

$$\text{Case 2: } E_t[\epsilon_{t+1}|R^m_{t+1}] = \alpha \neq 0, \tag{6}$$

$$\text{Case 3: } E_t[\epsilon_{t+1}|R^m_{t+1}] = g(R^m), \quad E_t[\epsilon_{t+1}] = \alpha \neq 0, \quad \text{Cov}_t(\epsilon_{t+1}, R^m_{t+1}) = 0, \tag{7}$$

where $g(\cdot)$ denotes a non-linear function. In the first case, any $M(R^m)$ that satisfies Equation (2) will also satisfy Equation (3), regardless of its functional form. (All proofs are provided in the internet appendix IA.1.1.) In the second case, ϵ contains one or several sources of systematic risk that are included in the unprojected pricing kernel and command additional risk premia beyond the market. But these risks are not related to R^m; thus, Equation (3) will not hold. In the empirical test below, book-to-market or profitability-sorted stock portfolios appear to be such an asset.

The third case is the one relevant for this paper. Here, the conditions specify that ϵ is nonzero in expectations and has a systematic but non-linear relationship with R^m. The conditions rule out that a linear $M(R^m)$ can price R^j, and $g(R^m)$ will show up in the pricing error alpha. A simple example of this case would be $\epsilon_{t+1} = (R^m_{t+1})^2$, with R^m following a symmetric distribution. However, a non-linear $M(R^m)$ could potentially capture the dependence $g(R^m)$ and hence price R^j. Formally, plugging the structure of R^j from Equations (4) and (7) into Equation (3) yields

$$E_t[M_{t+1}R^j_{t+1}] = E_t[M_{t+1}\beta^j R^m_{t+1}] + E_t[M_{t+1}g(R^m)] \tag{8}$$

$$= 0 + E_t[M_{t+1}g(R^m)]. \tag{9}$$

The last term in Equation (9) will be nonzero for a linear pricing model under the assumptions of Case 3, but can be zero if $M(R^m)$ is inversely related to $g(R^m)$. (IA.1.1 provides an example.)

In other words, for non-linear pricing to be relevant, one has to find a systematic, non-linear relationship $g(R^m)$ between the CAPM pricing errors ϵ and R^m, that is in addition inversely related to $M(R^m)$, i.e., covary with plausible sources of risk. The remainder of this section will show the first property in the data, and I will examine the second property in the Sections IV and V.

Finally, the Case 3 can have two different economic mechanisms and interpretations: either $M(R^m)$ solely captures how market risk is priced in a non-linear way, or there is a second priced risk factor that has a non-linear dependence with R^m such as, e.g., variance risk. The empirical and theoretical results in Sections V and VI, respectively, point toward the second interpretation.

B. Empirical curvature patterns: Example

I will illustrate the Case 3 from above using the example of the idiosyncratic volatility (Ivol) anomaly of Ang et al. (2006b), which refers to the empirical fact that portfolios comprising stocks with high Ivol have negative CAPM alphas, and vice versa (the next section provides more detailed information on the data). To motivate my measure for the non-linearity of $g(R^m)$ I draw on the key stylized property from the option-implied pricing kernel estimation in Section III.B below, namely, that the empirical estimates of $M(R^m)$ are predominately U-shaped. The simplest way to represent this property is

$$M_{t+1}^{approx} = a + b \times R^m + c \times (R_{t+1}^m)^2. \tag{10}$$

In Equation (10), the third term specifies the deviation from the linear CAPM; thus, the implied non-linearity is $g(R^m) \equiv (R_{t+1}^m)^2$, which measures curvature in returns.[4]

To quantify the curvature patterns, I first run the standard CAPM regression for each portfolio j of the 10 Ivol-sorted portfolios:

$$R_{t+1}^j = \alpha^j + \beta^j \times R_{t+1}^m + \epsilon_{t+1}. \tag{11}$$

[4]My measure of curvature is related to the coskewness measure of Harvey and Siddique (2000). I emphasize that it is merely a means to illustrate both the pervasive deviations from a linear relationship and the systematic relationship between tail exposure and CAPM alphas. Using the measure does not imply or assume that coskewness is the true pricing model. In fact, one obtains similar results when using alternative measures for $g(R^m)$, such as a piece-wise linear function, a quartic $(R^m)^4$-term, or sensitivity to realized variance. I prefer to use the quadratic $g(R^m)$ to capture co-movement in both tails due to its simplicity. In contrast to prior studies, I do not use any of these measures for pricing or for quantifying risk premia. Instead, the risk premia are inferred from the options market. Hence, I use the term "curvature" instead of "coskewness" to highlight the different interpretation of the relationship.

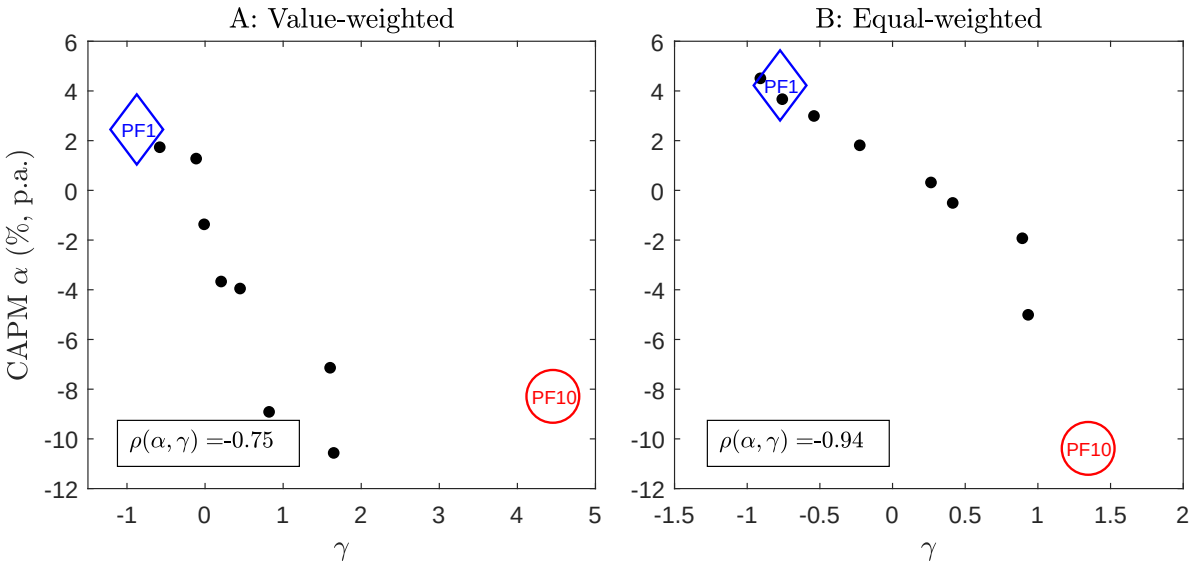

Figure 2: **CAPM alphas and curvature for Ivol-sorted portfolios.** The figure plots the estimated CAPM alphas from Equation (11) against the estimated γ coefficients from Equation (12). Panel A shows results for value-weighted returns of the Ivol-sorted stock portfolios, and Panel B shows the equal-weighted analog. The blue diamonds mark the first portfolio composed of the low-Ivol stocks, and the red circles indicate the 10th portfolio, which contains the high-Ivol stocks at each date. The correlation between the alphas and γs is shown in the bottom left of each plot. Returns are monthly, and the time period is 1996–2019.

I then run the CAPM regression extended by a square term on the market return:

$$R^j_{t+1} = constant + \tilde{\beta}^j \times R^m_{t+1} + \gamma^j \times \left(R^m_{t+1}\right)^2 + \epsilon_{t+1}. \tag{12}$$

The additional γ parameter measures the curvature of the relationship between R^j and R^m.

Figure 2 illustrates the results, which show a strong negative relationship between a portfolio's CAPM alpha and its curvature γ. The high-Ivol portfolio has a highly positive curvature and thus tends to outperform relative to the CAPM when the market has either large negative or large positive returns, while the opposite is true for the low-Ivol portfolio. Hence, the CAPM errors indeed have a non-linear relationship $g(R^m)$ that is inversely related to the pricing kernel in Equation (10).

This curvature pattern, which is illustrated in Figure 1, has an analog in the options market: the low-Ivol portfolio qualitatively resembles the payoff of a short straddle, while the high-Ivol portfolio resembles a long straddle. Empirically, it is well-documented that the low-Ivol portfolio as well as short straddles earn excess returns relative to the CAPM on average, while the opposite

is true for high-Ivol and long straddles. In the presence of a U-shaped $M(R^m)$, the low-Ivol portfolio is particularly risky, while the high-Ivol portfolio offers a hedge. To foreshadow the results, this property is exactly what the option-implied pricing kernel below will capture and price correctly.

C. Evidence for equities and other asset classes

C.1. Approach and Data

Starting with US equities, my goal is twofold. On the one hand, I want to identify and study prominent anomalies that have strong curvature patterns. I start with the 95 sorting variables considered in Gu et al. (2020). While I will discuss the results in more detail later, for now, to motivate my sample selection, I note that most portfolio sorts that use a sorting variable based on market data (stock returns and trading volume) have strong negative curvature patterns, while accounting data-based sorts do not. From those sorts with negative curvature patterns, I select the most prominent anomalies and include the remainder in the internet appendix. On the other hand, I want to study other prominent anomalies without any curvature pattern, i.e., well-known accounting-based anomalies.

As a result, my benchmark data include portfolios of stocks sorted on their CAPM beta (sometimes referred to as "betting-against-beta"), volatility (Vol) and idiosyncratic volatility (Ivol) as in Ang et al. (2006b), past maximum daily returns (Max) as in Bali et al. (2011), 12m-1m momentum as in Jegadeesh and Titman (1993), turnover (Turn) as in Datar et al. (1998), and days with zero trading volume (Ztrade) as in Liu (2006). Finally, I add beta w.r.t. daily changes in the VIX index ($\beta_{\Delta \text{VIX}}$) as in Ang et al. (2006a) because the idea behind their variable is to measure exposure to systematic variance risk, which is related to the variance-risk based explanation in this paper.

As further common test assets that largely do not have any curvature patterns, I include portfolios sorted on size, the book-to-market ratio (B/M), investment (Inv), profitability (Prof), accruals (Acc), and industry portfolios, each calculated following the definition on Kenneth French's website. Return data are from CRSP, accounting data from COMPUSTAT, and factor returns are taken from Kenneth French's website. Returns are monthly and calculated such that they match the timing of the option expiration. For each variable, I sort stocks into decile

portfolios. Appendix D contains further details about the calculation of characteristics and the portfolio formation.

To get more out-of-sample evidence, I use international stock market data. This sample is from the Compustat Global Securities database and comprises 16 developed European markets.[5] I focus on European countries because my approach requires a representative stock market index as well as an active options market to calculate the option-implied pricing kernel. All values are in USD, and the European factor data are again obtained from Kenneth French's website. The data are from 2002 to 2019, which matches the available EuroStoxx 50 options data.

For options, I construct four straddle portfolios with initial moneyness $K/S_0 \in \{0.90, 0.95, 1.00, 1.05\}$. For each month, I use the S&P 500 call and put option with moneyness closest to the target moneyness. For the portfolios in which one of the two options is in-the-money, I verify that the recorded option prices are very close to a synthetic option price calculated using the implied volatility of the second, out-of-the-money option. Because both excess returns of long straddles and their CAPM alphas are negative on average, I consider a short position. Straddles are particularly suited to studying the tail exposure because they naturally have a strong convex return relationship with the market.[6]

For commodities, I use returns to commodity spot indices from the Commodities Research Bureau, obtained from Bloomberg. This dataset includes the Spot Index and six subindices on metals, textiles, industrials, foodstuffs, fats and oils, and livestock.

C.2. Results

To quantify the curvature patterns, I first run regressions (11) and (12) for each portfolio. Then, for equities, I calculate the correlation between α^j from Equation (11) and γ^j from Equation (12) across the 10 portfolios of each strategy, both for value-weighted (VW) and equal-weighted (EW) portfolios. For options and commodities, I calculate the correlation across the respective four and seven portfolios.

[5]The countries are Austria, Belgium, Denmark, Finland, France, Germany, Great Britain (the United Kingdom), Italy, Ireland, Luxembourg, the Netherlands, Norway, Portugal, Spain, Sweden, and Switzerland.

[6]Note that the fact that M is derived from the same options data does not necessarily imply that M prices these returns correctly. Only if the return density $f_t(R_{t+1})$ used for the estimation in (13) below is the true one, or at least close to it, M will also price option returns.

Table 1: **Curvature Patterns for Various Asset Classes**

Panels A–E show the correlation coefficient $\rho(\alpha, \gamma)$ between the CAPM alpha from (11) and the curvature parameter γ from (12) across portfolios in the first row of each panel. For equities, the correlation is calculated across the 10 portfolios of each sort. VW denotes value-weighted portfolios, and EW denotes equally-weighted portfolios. For options and commodities, the curvature is calculated across the respective four and seven portfolios. For a more detailed description of the portfolio calculation, see Appendix D. Panel F shows the magnitude of curvature parameters γ from Equation (12) for the VW portfolios from Panel A. The first two rows show the lowest and highest γ for each sort, and the last row shows the γ for the high-minus-low (HML) portfolio. t-statistics (in parentheses) are adjusted for heteroscedasticity and autocorrelation (Newey and West 1987).

Panel A: US Equities with Curvature Patterns								
	Beta	Vol	Ivol	Max	Mom	Turn	Ztrade	$\beta_{\Delta\text{VIX}}$
VW	-0.75	-0.85	-0.73	-0.94	-0.76	-0.68	-0.70	-0.75
EW	-0.99	-0.96	-0.93	-0.95	-0.89	-0.97	-0.96	-0.94
Panel B: Other Equity								
	Size	B/M	Inv	Prof	Acc	Industry		
VW	0.61	-0.10	-0.43	0.29	-0.28	-0.54		
EW	0.06	-0.08	-0.58	-0.25	-0.12	0.03		
Panel C: European Equity								
	Beta	Vol	Ivol	Max	Mom	Turn	Ztrade	$\beta_{\Delta\text{VIX}}$
VW	-0.78	-0.89	-0.71	-0.83	-0.80	-0.66	-0.70	-0.77
EW	-0.97	-0.97	-0.96	-0.95	-0.94	-0.89	-0.89	-0.76
Panel D: Options				Panel E: Commodities				
	-0.63				-0.88			
Panel F: Magnitude of Curvature Patterns for VW from Panel A								
	Beta	Vol	Ivol	Max	Mom	Turn	Ztrade	$\beta_{\Delta\text{VIX}}$
Min(γ)	-1.50	-1.57	-0.87	-1.57	-0.79	-1.32	-1.00	-0.78
	(-4.01)	(-4.25)	(-3.15)	(-5.61)	(-4.63)	(-4.56)	(-3.58)	(-2.32)
Max(γ)	2.05	2.75	4.45	2.51	3.01	1.48	1.41	1.23
	(2.36)	(3.21)	(6.11)	(3.93)	(2.28)	(2.51)	(2.45)	(2.21)
γ^{HML}	-3.55	-4.32	-5.33	-4.02	-2.59	-2.16	-1.89	-1.30
	(-3.75)	(-4.63)	(-6.83)	(-5.46)	(-1.66)	(-3.22)	(-2.81)	(-1.75)

The results in Panel A of Table 1 show that for portfolios sorted on Beta, Vol, Ivol, Max, Mom, Turn, Ztrade, and $\beta_{\Delta\text{VIX}}$, there is a strong negative correlation between the portfolios' α and γ. Furthermore, the correlation is stronger for equal-weighting and often close to -1.

To appreciate the economic magnitude of these patterns, Panel F in Table 1 presents the γ^{HML} of the high-minus-low (HML) portfolio. Consider, for example, the case of Ivol. The

$\gamma = -5.3$ implies that when $R^m = \pm 10\%$, the Ivol HML portfolio is expected to underperform the linear relationship by $-5.3 \times 0.1^2 = -5.3\%$, and for a relatively large $R^m = \pm 20\%$, the non-linearity amounts to $-5.3 \times 0.2^2 = -21.1\%$ per month.

The documented correlation between alpha and curvature across portfolios confirms that there is a systematic pattern and that these sorts are systematically related to an additional source of risk besides the linear market factor. If a negative γ^{HML} occurred simply by chance, it would likely not appear jointly with the correlation pattern across all 10 portfolios. On the flip side, a few sorts exhibit a correlation pattern but have an insignificant γ^{HML} . This result could stem from a non-monotonic exposure across portfolios, and the online appendix presents an example.

Another interesting insight from Panel F of Table 1 is that the sorts based on $\beta_{\Delta \text{VIX}}$ exhibit the lowest γ^{HML}. This finding is surprising because $\beta_{\Delta \text{VIX}}$ should measure an exposure to systematic variance, suggesting one should expect strong dependence in the tails of the return distribution. Section V revisits this point and shows the extent to which $\beta_{\Delta \text{VIX}}$ indeed measures exposure to (monthly) systematic variance risk.

Panel B of Table 1 shows that for size, book-to-market, profitability, and accruals portfolios, there is no, or even a positive, relationship between α and γ. For investment and industry-sorted portfolios, I find a negative relationship for the value-weighted portfolios, but it is not as strong as for the sorts in Panel A. Turning to European stocks, the results in Panel C confirm the $\alpha - \gamma$ correlation pattern found in US data. Lastly, Panels D and E document the same results for options straddles and commodities. While several studies have documented downside dependence for some anomalies (e.g., Boguth et al. 2011; Lettau et al. 2014), the novel result here is the upside dependence. Moreover, Table IA.4 documents that the curvature patterns are also obtained when estimating a piece-wise linear function that allows for different coefficients for upside and downside dependence, emphasizing that the relationship is really convex/concave in both tails and not mechanically induced by the $(R^m)^2$ term.

Finally, I look at the curvature patterns in the full set of all 95 sorting variables considered in Gu et al. (2020). The results, presented in Table IA.1, paint an interesting picture. No accounting-based sorts, which are the vast majority of sorts, display a strong negative curvature pattern. In contrast, most sorts based on market data (returns and volume) do have strong negative curvature patterns. In addition to the variables studied in Panel A of Table 1, this

analysis includes several other measures of momentum and stock liquidity. In total, 16 of the 22 sorts that use only market data have strong curvature patterns. Moreover, the other six sorts in this group have low and insignificant alphas in the sample, and hence my model would also not predict them to have significant curvature patterns.

III. Pricing Kernel Estimation

This section briefly explains the approach for estimating the pricing kernel as a function of stock market returns and how I estimate conditional risk-neutral and physical return densities. I then discuss data sources and present the estimation results.

A. Approach

It is well known that the absence of arbitrage implies the existence of a pricing kernel, or stochastic discount factor, that prices all assets. This paper studies the (non-linear) projection of the pricing kernel onto stock market returns, defined as

$$E_t[M_{t+1}|R^m_{t+1}] = \frac{1}{R^f_t}\frac{f^*_t(R^m_{t+1})}{f_t(R^m_{t+1})}, \tag{13}$$

where $f^*_t(R^m_{t+1})$ and $f_t(R^m_{t+1})$ denote the conditional risk-neutral and physical density of the ex-dividend market excess return R^m_{t+1}, respectively, and R^f_t is the gross risk-free rate. This object is the expected value of the pricing kernel in $t+1$, conditional on observing a given return R^m_{t+1}; hence, $M(R^m)$ is only a function of R^m. For brevity, I use the shorthand notation M to denote the ex ante expectation and M_{t+1} to denote realizations. Furthermore, M without the superscript represents the option-implied estimate from Equation (13), and I use specific superscripts to denote alternative specifications.

To estimate f^* and f, I use standard tools from the literature, which I next briefly summarize, while the technical details and descriptive statistics of the data are provided in Appendix A. First, for each month, I extract f^* from S&P 500 option prices using the classical results of Banz and Miller (1978) and Breeden and Litzenberger (1978). This method is standard, and the obtained densities are truly conditional as they reflect only option information from a given point in time. The data are from OptionMetrics and cover 1996 to 2019. Second, to construct f, I use a method often referred to as "filtered historical innovations," which is semi-parametric and the most common methodology in the literature on pricing kernel estimation.[7] Data are daily S&P 500 returns obtained from CRSP.

[7]See, e.g., Rosenberg and Engle (2002), Barone-Adesi et al. (2008), Christoffersen et al. (2013), Faias and Santa-Clara (2017), and Christoffersen et al. (2022).

Third, to make f_t a conditional density, I require a conditional volatility forecast. Because volatility is a key ingredient for the estimation of M (Sichert 2023), I require a good model to forecast it.

An extensive econometric literature studies volatility modeling and forecasting. By now it is generally understood that models based on high-frequency realized variances (RV) outperform other models, as e.g., the standard GARCH models. I follow Bekaert and Hoerova (2014) and compare out-of-sample performance of numerous state-of-the art RV models for the S&P 500 at the one-month horizon. The best RV model contains realized jumps and the VIX as predictors. The details of the model specification and estimation are provided in the Appendix B, and alternative RV models are included in the robustness Section IV.F.

Throughout the paper, I will refer to the variance forecast from t to $t+1$ (21 trading days) as the expected variance over the next month, denoted as σ_t^2. Lastly, note that all quantities in Equation (13) are calculated in a rolling-window fashion, i.e., using only data available up to date t, and thus M is estimated in real time.

The benchmark approach estimates f^* only over the range of strikes for which options data exist. In the sample, the realized return is never lower than the lowest observed strike; therefore, the extrapolation of the left tail is not relevant for the pricing results below. However, high positive returns do exceed the highest observed strike nine times in the sample, on average by 1.2 percentage points. Therefore, a robust way of extrapolating either f^* or M in the right tail of the distribution is required. My benchmark approach is to simply extrapolate the observed M linearly. Alternatively, I use the ratio of the cumulative return density in the tails that is not covered by the options data, formally expressed as

$$M(R^{right\ tail}) = \Big(1 - F_t^*\big(R_{t,t+1}^{max}\big)\Big) / \Big(1 - F_t\big(R_{t,t+1}^{max}\big)\Big). \tag{14}$$

In Equation (14), R_{t+1}^{max} corresponds to the highest available strike at date t, and F denotes the cumulative density function (CDF). This ratio provides an indication of the behavior of M in the tail, and it can be interpreted as the average M in that region.

These approaches to extrapolating M are more robust than extrapolating f^* by "tail fitting," which makes the estimated M in the tail strongly dependent on guessing the right parametric distribution for the tails. I test alternative ways to extrapolate M – as well as f^* – in the

robustness Section IV.F.

B. Estimation results

Figure 3 presents the estimated pricing kernels M for each month, grouped by the 24 years in the sample. The pricing kernel estimates are relatively steep on the left and predominately U-shaped. The U-shape is most pronounced in times of high market volatility, e.g., around the 2000s and during the financial crisis and its aftermath, 2008–2011. In times of low volatility, the estimates sometimes have a hump around zero, likely caused by the volatility forecast being too high. (See Sichert (2023) for a more detailed discussion of this issue.) This hump is most pronounced in the years 2017 and 2018, when both market volatility and the VIX were at their all-time low, lending support to this argument. Such an all-time low in volatility is hard to capture with an out-of-sample prediction, where the model never saw these low levels in the estimation. Nevertheless, most estimates M trend upward toward their right tail.

The steepness of M on the left is consistent with the highly negative returns to S&P 500 put options (Broadie et al. 2009, among others). The increasing part on the right is consistent with the negative average returns of out-of-the-money S&P 500 call options (Bakshi et al. 2010). In the literature on the cross-section of stock returns, the steepness of M on the left is consistent with evidence on the importance of downside risk. In contrast, the implications for stock returns of the increasing part on the right has received little attention, but will be the focus of the analyses that follow.

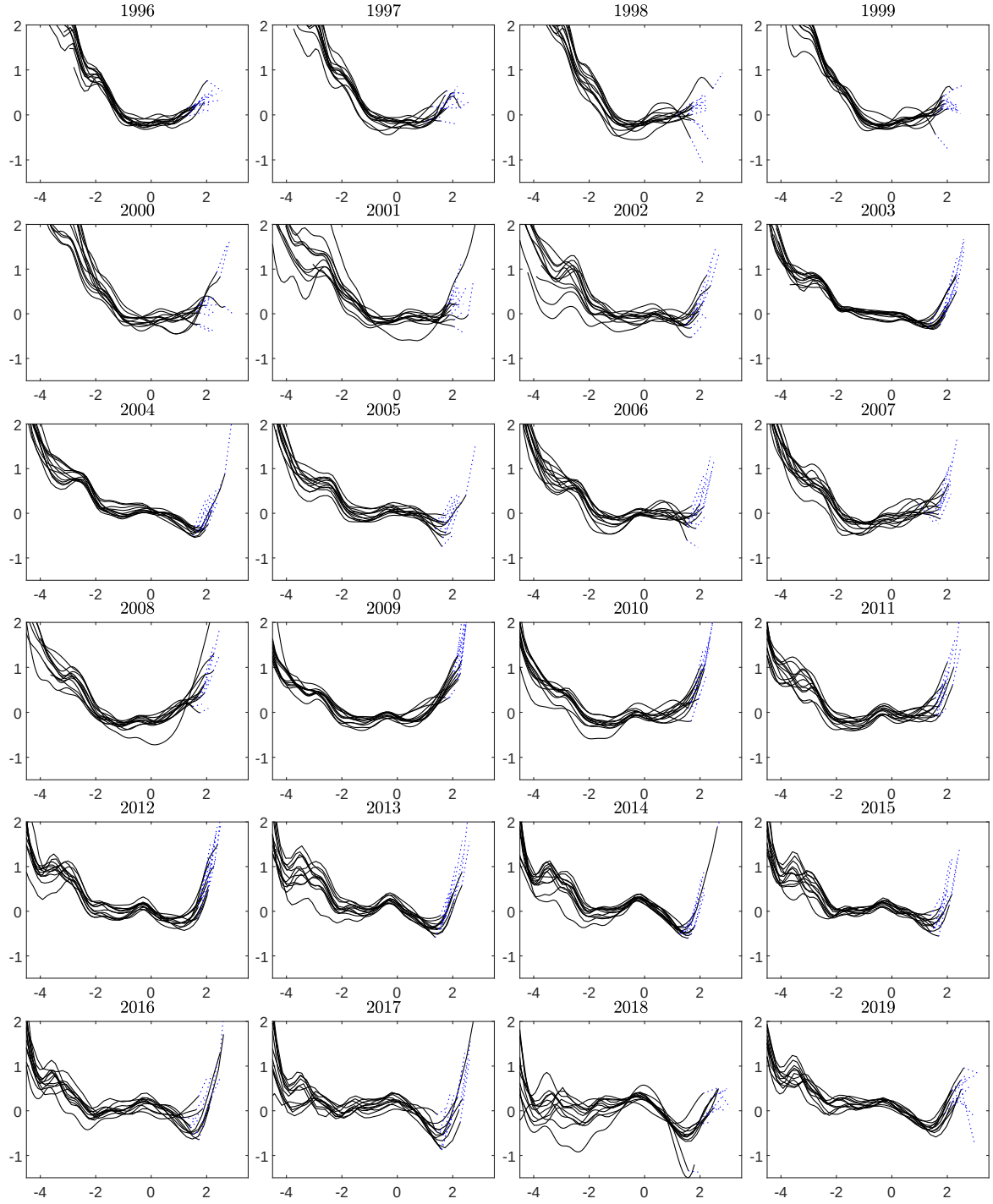

Figure 3: **Pricing kernel estimates.** The figure shows the natural logarithm of estimated pricing kernels. Standardized returns $= R^m_{t+1}/\sigma_t$ are on the horizontal axis. The horizon is one month. The dotted blue line connects the points, which depict the ratio of the CDFs of the tail from Equation (14), with the corresponding pricing kernels.

IV. Pricing Results

A. Approach

To test the pricing performance of M, I study Euler equation errors, a nonparametric and standard way to test a candidate pricing kernel (see, e.g., Cochrane 2005; Parker and Julliard 2005). Euler equation errors can economically be interpreted as pricing errors and are commonly referred to as "alphas." The Euler equation reads

$$E_t[M_{t+1}R^j_{t+1}] = 0 \tag{15}$$

for the excess return R^j of each asset j. Empirically, I calculate alphas as

$$\alpha^j = \frac{1}{T}\sum_{t=1}^{T} M_{t+1}R^j_{t+1}. \tag{16}$$

The series of realized M_{t+1} is calculated as described in Section IV.C below. Note that the alphas for factor models from Equation (16) are virtually the same as from the more common regression-based model tests.[8]

To compare the pricing results to standard benchmark models, I also calculate the alphas of the CAPM and the Fama and French (1993) three-factor model (FF3). The pricing kernel in the CAPM is a linearly decreasing function of the market return. Also, the FF3 model is virtually monotonically decreasing in the index, as the other two factors are virtually orthogonal to the market (as depicted later in Figure 5D). Finally, I consider the coskewness (CoSkew) factor of Harvey and Siddique (2000) in addition to the market. See Appendix C.2 for details on the calculation of the pricing kernel in the linear factor models.

As test assets, I use the portfolios described in Section II.C.1. For each strategy, I form the high-minus-low (HML) portfolio such that the strategy produces a positive CAPM alpha. In most cases, this strategy also maximizes the curvature exposure. Because industry portfolios have no natural HML sorting, I go long (short) the portfolio with the highest (lowest) in-sample

[8]To be precise, $\alpha^{\text{Euler}} = \alpha^{\text{regression}}/R_f$. IA.1.3 shows this relationship for the CAPM. A general proof can be found in Dahlquist and Söderlind (1999). Note that an advantage of the Euler equation approach is that it allows for risk premia and exposures to be time-varying, without having to specify the nature of the time-variation.

CAPM alpha, to keep the analysis simple. All portfolios are value-weighted in the benchmark analysis.

For commodities, I form a long-short portfolio that maximizes CAPM alpha (as well as curvature), going long the portfolio with the highest CAPM alpha and short the one with the lowest CAPM alpha. Finally, since all straddles have negative curvature, I take a short position in the at-the-money straddle financed at the risk-free rate, which has both the highest CAPM alpha and the most negative curvature.

B. Monotonically decreasing pricing kernel and upside risk

To isolate the increasing part of M, and therefore the upside-risk premium, I calculate a strictly monotonic decreasing counterpart M^{mon} for each estimated M. Figure 1 illustrates this relationship, with the solid black line extended by the dotted line to the right of the minimum. To be precise, for a given estimate M, I first find the global minimum in the area of positive returns. Next, graphically speaking, I discard the entire estimate to the right of this minimum, and then linearly extrapolate the remainder using the slope coefficient from the CAPM. The difference in pricing errors between M^{mon} and M for an asset measures its upside risk premium. Formally,

$$\text{Upside risk premium}^j = \frac{1}{T}\sum_{t=1}^{T}\Big(M_{t+1}^{mon} - M_{t+1}\Big)R_{t+1}^{j}. \tag{17}$$

A formal derivation of the relationship is provided in IA.1.2.

C. Realized pricing kernel

To assess the pricing performance of M using Equation (16), one needs to calculate a realized M. Each line in Figure 3 is an ex ante functional form that describes how the random future realized R_{t+1}^{m} maps into a realized M_{t+1}. Hence, for each observed return R_{t+1}^{m} from date t to $t+1$, there is a corresponding realized M_{t+1}. Figure 4 illustrates this mapping for a selected date. The ex ante M was calculated on June 18, 2008. The observed log return on July 19, 2008, was -5.50%, which corresponds to a realized $M_{t+1} = \exp(-0.22) = 0.80$.

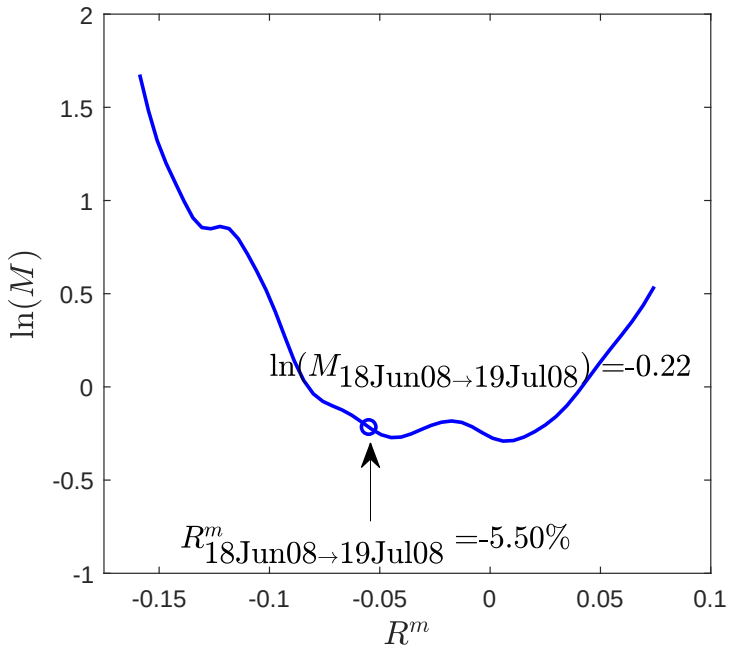

Figure 4: **Calculation of realized pricing kernel.** The figure illustrates the calculation of the realized pricing kernel on a selected date.

D. Results for US equities

For the pricing of equities, I split the analysis into strategies that have a strong $\alpha-\gamma$ correlation and those that do not. Table 2 presents the main pricing results for both groups. I follow Burnside (2011) and bootstrap statistical significance.[9] The first column in Panel A shows that the option-implied M prices all tabulated anomalies. The alphas are economically low and statistically insignificant. The second column shows the estimated upside risk premium. For all anomalies, this upside risk premium is large, between 29% of the CAPM alpha in the case of $\beta_{\Delta\text{VIX}}$ and 89% for the low beta anomaly. On average, the upside risk premium is 4.0% per annum (p.a.) and almost half of the CAPM alpha. Furthermore, the upside risk premium is always statistically significant. Hence, it is an important risk factor for understanding the returns to those portfolio sorts.[10]

[9]Specifically, I use $N = 50,000$ i.i.d. bootstrap draws. The draws are i.i.d. because the Ljung-Box test at lags up to 30 rejects auto-correlation in the time series. I verify for the CAPM and the FF3 model that the bootstrapped p-value is similar to (and often more conservative than) a regression-based p-value obtained using Newey and West (1987) adjusted standard errors.

[10]By construction, the remaining difference between M^{mon} and the CAPM stems from the remaining non-linearity in M^{mon}, which is mostly driven by the steep slope in the left tail. Thus, the average difference between upside risk and CAPM alpha can be interpreted as compensation for the downside

Table 2: **Pricing Results for Equity Portfolios**

The table shows the pricing errors (alphas) for M, the CAPM, the Fama and French (1993) three-factor model (FF3), and the CAPM plus the coskewness factor of Harvey and Siddique (2000), all calculated via Equation (16). The table also shows the upside risk premium (RP), calculated via (17). Returns are from the high-minus-low value-weighted portfolios. The symbols ***, **, and * indicate that values are significantly different from zero at the 1%, 5%, and 10% significance levels, respectively. The significance levels are obtained from 50,000 (pairwise) bootstrap draws from the sample of alphas (differences in alphas). All numbers are annualized in percentages.

	M	Upside RP	CAPM	FF3	CoSkew
Panel A: Equity Portfolios with Curvature Patterns					
Beta	-0.65	6.26***	7.02	8.03*	4.83
Vol	3.01	5.15***	11.29**	11.18**	8.83*
Ivol	2.92	4.44***	10.74**	10.30*	8.57*
Max	1.14	3.80***	8.05*	7.43*	6.24
Mom	1.65	3.73***	10.39*	13.09**	10.15*
Turn	3.88	3.41***	8.54**	7.33*	5.86
Ztrade	4.00	3.14***	8.36**	7.33**	6.24*
$\beta_{\Delta \text{VIX}}$	3.17	2.04***	6.91**	7.00**	5.40*
Avg	2.39	4.00***	8.91**	8.96**	7.02**
Panel B: Other Equity Portfolios					
Size	1.20	0.10	-0.01	-0.39	0.24
B/M	1.53	-1.19**	1.19	-2.75	0.47
Inv	3.60	-0.68	3.50*	2.20	3.09
Prof	5.90***	0.25	6.44***	6.74***	6.11***
Acc	3.55*	0.04	3.65**	3.59**	3.77**
Industry	5.90	2.81***	7.90*	8.60**	5.69

The third and fourth columns of Table 2, Panel A show the CAPM and FF3 alphas, respectively. Not all of the values are statistically significant for two reasons. First, as expected, the level of alphas is lower than in previous studies, since it is well-known that alphas of many anomalies decrease in the later sample. In addition, the bootstrap tends to be conservative relative to using Newey and West (1987) adjusted standard errors from regressions, and this tendency is particularly true for the FF3 model.[11] Nevertheless, the average alpha is significant

risk exposure of the anomalies. The average value the downside risk premium of $8.91\% - 4.0\% = 4.91\%$ is well in line with the 6% estimated in Ang et al. (2006a).

[11]This tendency can, for example, be seen when considering that a regression based the FF3 test leads to a t-statistic of 2.77 for Vol, 2.88 for Ivol, and 3.10 for the average alpha, which would all be significant at the 1% level. Furthermore, this study uses open prices from the third Friday of the month to match the option expiry timing. Using closing prices at the settlement dates would increase annual alphas, on average, by 2 percentage points and t-statistics by 1. These results are consistent with Polk et al. (2019), who document that anomalies accrue mostly during trading hours and have the opposite sign overnight.

at the 5% level for both the CAPM and FF3. Furthermore, the pricing error of M is always much lower than those of either the CAPM or FF3 (and the difference is statistically significant, see Table IA.5).

The last column of Table 2, Panel A shows that the CAPM plus coskewness factor cannot price most of the anomalies. The decrease in alpha for Beta, Vol, and Ivol is consistent with the results in Schneider et al. (2020). Nevertheless, many other alphas do not decrease relative to the CAPM, and the average alpha is significant at the 5% level.

Switching attention to Panel B of Table 2, one can make several observations. First, some prominent sorts, such as size, B/M, and investment, have relatively low alphas in the recent sample, which has already been documented in the literature. Second, M prices all portfolios similarly well, compared to the factor models. For Size, B/M, Inv, Prof, and Acc, the pricing errors for M are very close to those for the CAPM and the FF3 model. For the industry portfolios, the pricing error of M is insignificant but relatively large. Furthermore, there is a significant upside risk premium of 2.8% p.a., which is about 32% of the CAPM alpha. This finding is consistent with both the negative correlation between α and γ in Table 1 and the findings of Dittmar (2002).[12] For all other portfolios, there is little evidence of upside risk, and the absence of any curvature pattern in Table 1 also would not imply and upside risk. Thus, the pricing errors of these accounting sorts appear to be "Case 2" from Section II.A.

In sum, given that M is estimated from options data only and without any cross-sectional stock return information, the results are very encouraging. The results further suggest that many anomalies are only anomalies for linear models and do not exist if the pricing kernel is allowed to be non-linear, or even non-monotonic, to capture upside risk.

E. Results for other asset classes

Next, I extend the analysis to the other asset classes and present the results in Table 3. For European equities, I calculate M analogously to the US, using options and return data for the EuroStoxx 50. The resulting M is again largely U-shaped (see Figure IA.1).

[12]Dittmar (2002) shows that a cubic $M(R^m)$ can price industry portfolios, but he notes that the resulting shape of M is inconsistent with standard utility theory. He further shows that imposing a monotonically decreasing $M(R^m)$ — that is consistent with standard utility theory — significantly worsens the pricing performance. Together, these results imply that upside risk is crucial for explaining the returns of industry portfolios, consistent with my results.

Table 3: **Pricing Results for European Equity, Option Straddles and Commodity Portfolios**

The table shows the pricing errors (alphas) for M, the CAPM, the Fama and French (1993) three-factor model (FF3), and the CAPM plus the coskewness factor of Harvey and Siddique (2000), all calculated via Equation (16). The table also shows the upside risk premium (RP), calculated via Equation (17). Returns are from the high-minus-low value-weighted portfolios. The symbols ***, ** and * indicate that values are significantly different from zero at the 1%, 5%, and 10% significance levels, respectively. The significance levels are obtained from 50,000 (pairwise) bootstrap draws from the sample of alphas (differences in alphas). All numbers are annualized in percentages.

	M	Upside RP	CAPM	FF3	CoSkew
Panel A: European Equity					
Beta	-2.51	6.72***	9.34**	8.83**	9.09**
Vol	1.61	5.91***	13.08***	14.42***	11.57***
IVOL	1.54	5.47***	12.68***	14.13***	11.15***
Max	-0.61	5.66***	10.50***	11.69***	9.18***
Mom	12.74**	6.04***	24.35***	25.40***	24.16***
Turn	3.52	6.19***	15.11***	15.39***	14.08***
Ztrade	3.35	6.19***	14.96***	15.25***	13.95***
$\beta_{\Delta \text{VIX}}$	0.98	3.65***	9.28***	10.79***	9.40***
Avg	2.58	5.73***	13.66***	14.49***	12.82***
Panel B: Options					
Straddle	-0.74	43.70***	81.42*	77.49*	78.37*
Panel C: Commodities					
HML	-1.16	3.50**	3.67	2.84	4.04*

Panel A of Table 3 shows that M again prices returns of portfolios sorted on Beta, Vol, Ivol, Max, Turn, and Ztrade. All alphas are close to zero and insignificant. In contrast, these portfolios have large and significant alphas relative to the CAPM and the FF3 model. Momentum is an exception, but the pricing error of M is still half that of the factor models. Moreover, the second column again shows a large and significant upside risk premium. On average, it is 5.7% p.a., or almost half of the CAPM and FF3 alphas.

The results in Panel B of Table 3 show that M also prices returns to short at-the-money S&P 500 straddles well. The pricing errors are virtually zero and insignificant. For the CAPM and the FF3 model, however, they are large and significant. Moreover, the second column reveals a large upside risk premium that is more than half of the CAPM alpha. While it is well known that the CAPM does not price option returns well, it is a new result that a substantial part of

the pricing error stems from upside risk. Finally, for commodities in Panel C, the results show insignificant pricing errors for M and a sizable and mildly significant upside risk premium.

F. Robustness

The main parametric input in the estimation of M is the return density and the variance forecast. I therefore test the robustness of the modeling choices made for the estimation of M and present the results in Table 4. For brevity, I focus on the equity portfolios with a pronounced curvature pattern and summarize the pricing performance by presenting the average alpha, i.e., the analogue to the line "Avg" in Panel A of Table 2. Overall, the results are fully robust to any of the choices made above. In all specifications, the pricing error for M is insignificant, and the upside risk premium is estimated to be between 2.5% and 4.9% p.a. Furthermore, in the cases in which the upside risk premium is estimated to be lower than the 4.0% of the benchmark approach, the difference stems from the fact that the M of the alternative approaches are less U-shaped (not tabulated).

First, I test alternative methods to extrapolate M in the tail. The first alternative uses Equation (14) to extrapolate M in the region of high positive returns. The second alternative uses the method suggested by Figlewski (2010) to "complete the tails" of $f^*(R)$ using a generalized extreme value (GEV) distribution.

Second, I test alternative approaches to model the physical density $f(R)$. One alternative is to use an extending window for the shocks Z in Equation (33) in Appendix A.3. A second alternative is to use the skew t distribution of Azzalini and Capitanio (2003). The parameters of the distributions are estimated with maximum likelihood. In addition, I make the parameters that control skewness and kurtosis linear functions of σ_t to account for the finding that higher moments vary with market volatility (Gormsen and Jensen 2022).

Third, I present the results for alternative variance models that rank behind the benchmark model in terms of variance forecasting accuracy (for details, see Appendix B). They are variations on the benchmark model that include either the VIX or jumps, or the estimation methodology is changed from weighted-least squares to ordinary least squares. Table 4 shows that the pricing errors for the alternative RV models slightly increase and the upside risk premium (as well as the U-shape of the estimated M, not tabulated) slightly decreases with the

Table 4: **Robustness Pricing Results for Equity Portfolios**

The table shows the pricing errors (alphas) for M, the CAPM, the Fama and French (1993) three-factor model (FF3), and the CAPM plus the coskewness factor of Harvey and Siddique (2000), all calculated via Equation (16). The table also shows the upside risk premium (RP), calculated via Equation (17). Returns are from the high-minus-low value-weighted (last row: equal-weighted) of all portfolios in Panel A of Table 2. For a description of the model details for each row, see the main text. The symbols ***, **, and * indicate that values are significantly different from zero at the 1%, 5%, and 10% significance levels, respectively. The significance levels are obtained from 50,000 (pairwise) bootstrap draws from the sample of alphas (differences in alphas). All numbers are annualized in percentages.

	M	Upside RP	CAPM	FF3	CoSkew
CDF extrapolation	3.44	3.81^{***}	8.91^{**}	8.96^{**}	7.02^{**}
GEV	3.50	2.54^{***}	8.91^{**}	8.96^{**}	7.02^{**}
$f(R)$ - extending window	2.39	3.05^{***}	8.91^{**}	8.96^{**}	7.02^{**}
$f(R)$ - Skew t	0.37	4.92^{***}	8.91^{**}	8.96^{**}	7.02^{**}
RV model w. VIX	3.71	3.18^{***}	8.91^{**}	8.96^{**}	7.02^{**}
RV model w. Jumps	3.39	3.51^{***}	8.91^{**}	8.96^{**}	7.02^{**}
RV model w. VIX, Jumps, OLS	3.54	3.71^{***}	8.91^{**}	8.96^{**}	7.02^{**}
$M^{weakly\ mon}$	2.27	2.83^{***}	8.91^{**}	8.96^{**}	7.02^{**}
EW portfolios	5.69	3.19^{***}	10.77^{***}	10.89^{***}	9.22^{**}

variance forecasting performance of the RV model.

Fourth, I calculate a weakly monotone M^{mon}, i.e., extrapolating to the right of the global minimum with a slope of 0. This decreases the average estimated upside risk premium by about 1.2 percentage point p.a. In other words, of the average 4.0% risk premium, 2.8% stems from the increasing part of M and 1.2% stems from the difference between a flat versus a decreasing M in the right tail.

Finally, I present the results for equal-weighted portfolios instead of value-weighted, as in the benchmark approach. All alphas increase, but otherwise the results do not change qualitatively.

V. A Variance Risk-Based Explanation

Variance risk is arguably the most important risk factor for options. This section shows empirically that variance risk is also important for explaining the cross-section of stock returns and that it induces a non-monotonic projected pricing kernel. Section VI then provides an equilibrium foundation for this reduced-form approach.

A. Variance risk and U-shaped M

On a general level, the U-shaped estimates for M in Figure 3 show that investors are averse to R^m realizations in both tails. In the option pricing literature, stochastic variance is arguably the most important risk factor for explaining option prices. Christoffersen et al. (2013) show that priced variance risk is a viable explanation for the U-shaped pricing kernel. Their model assumes a pricing kernel that is decreasing in R^m and increasing in variance. The latter feature generates the empirically well-documented variance risk premium. In addition, their model assumes a U-shaped relationship between variance and returns, which I confirm empirically below. Together, these assumptions give rise to the U-shaped projection. The structural model in Section VI provides an equilibrium foundation for this reduced-form modeling approach.

To test the mechanism empirically, I augment the CAPM with a variance factor. Fortunately, variance risk is a traded asset. Specifically, it is well known that the VIX^2 is the price of a variance swap with 30 days to maturity.[13] Because the VIX is calculated as the forward price, I convert it into the spot price VIX^2/R_f, which is equivalent to the price of the replicating options portfolio. The pricing kernel then reads

$$M_{t+1}^{VS} = a_t + b_t \times R_{t+1}^m + c_t \times \left(\frac{RV_{t+1}^{(21)}}{VIX_t^2/R_{f,t}} - R_{f,t} \right), \tag{18}$$

where $RV_{t+1}^{(21)}$ denotes the realized monthly variance of the market index from time t to $t+1$.

[13] Although strictly speaking, VIX^2 is only a close approximation, it has become standard in the literature to use the VIX as a proxy for the price of the swap. See, for example, Cheng (2019) for a detailed discussion of this issue. Furthermore, using a proprietary data set of quoted prices for S&P 500 variance swaps with one month maturity ranging from January 1996 to October 2013, I verify that the VIX^2 is a close approximation of the actual variance swap rate. The two series have a correlation of 99.1%, and the average level of swap rates is 21.2% compared to an average VIX of 21.6% (both in VIX units).

Consequently, the last term mimics the excess return on a variance swap (VS).[14]

After plugging Equation (18) into Equation (1) and conditioning down, I obtain an expression for expected returns that can then be tested using the following regression:

$$R^j_{t+1} = \alpha^j + \beta^j \times R^m_{t+1} + \gamma^j \times \left(\frac{RV^{(21)}_{t+1}}{VIX^2_t/R^f_t} - R^f_t \right) + \epsilon_{t+1}. \tag{19}$$

Panel A of Table 5 presents the results for each HML equity portfolio, with t-statistics based on Newey and West (1987) adjusted standard errors. The results show that adding the variance factor to the CAPM decreases the alphas significantly: all presented alphas are statistically insignificant, and the average decreases to 3.58% p.a. from 8.91% p.a. in Table 2. The last column shows that the estimated γ coefficients are negative for each long-short portfolio. To understand the economic magnitude, note that the average excess return of the variance swap factor is -26.44% per month. Hence, the γ for the average anomaly return of -0.0161 implies a premium for systematic variance exposure of $-0.0161 \times -26.44\% = 0.426\%$ per month, or 5.11% p.a. The highest variance risk premium is found for momentum with $-0.0406 \times -26.44\% = 1.07\%$ per month, or 12.88% p.a.

Panel B of Table 5 shows results for European equities. Once again, the alphas decrease substantially, rendering them all insignificant. The estimated γ coefficients are similar in magnitude to the results using the US return data. Furthermore, the pricing error for at-the-money S&P 500 options straddles in Panel D is an insignificant -45.75% p.a., relative to a significant 81.42% p.a. for the CAPM in Table 3. The estimated exposure to variance risk, γ, is large and significant, which is not surprising given the abundant evidence that options, and in particular straddles, are heavily exposed to variance risk.

Overall, a simple extension of the CAPM with a priced variance factor leads to a pricing performance that is similar to that of the option-implied M. To dissect the pricing performance, Figure 5 sheds light on the relationship between R^m and different measures for realized variance.

[14]While different approaches can be used to calculate the payoff of a variance swap, the most common one in the literature is to use squared daily log returns. This paper uses five-minute returns throughout because this measurement is widely recognized to deliver a more precise estimate of RV. Because the average RV from high-frequency returns is lower than that obtained from squared daily returns, I scale my RV to be at the same level on average, making my results comparable to those of other studies. Nevertheless, using squared daily returns to calculate the payoff delivers very similar results (see Table IA.6).

Table 5: **CAPM + Variance Swap Pricing Results for Equity, European Equity, Commodity and Option Portfolios**

The table shows alphas from regression (19), annualized in percentages. t-statistics (in parentheses) are adjusted for heteroscedasticity and autocorrelation (Newey and West 1987). The estimated γ coefficients are multiplied by 100 for readability.

	α		β		$\gamma \times 100$	
Panel A: Equity						
Beta	-0.04	(-0.01)	-1.28	(-10.35)	-2.15	(-1.58)
Vol	5.64	(1.09)	-1.32	(-8.21)	-1.57	(-1.59)
Ivol	4.74	(0.72)	-1.16	(-6.11)	-1.79	(-1.41)
Max	2.94	(0.52)	-1.00	(-7.44)	-1.52	(-1.40)
Mom	-0.92	(-0.10)	-0.88	(-4.22)	-4.06	(-2.50)
Turn	6.70	(1.55)	-0.86	(-8.84)	-0.28	(-0.37)
Ztrade	5.01	(1.32)	-0.85	(-9.04)	-0.89	(-1.39)
$\beta_{\Delta \text{VIX}}$	4.60	(1.43)	-0.52	(-6.30)	-0.65	(-0.96)
Avg	3.58	(0.97)	-0.98	(-8.98)	-1.61	(-2.11)
Panel B: European Equity						
Beta	-6.83	(-0.57)	-0.85	(-9.73)	-2.48	(-1.48)
Vol	2.24	(0.16)	-0.53	(-3.41)	-1.48	(-0.69)
Ivol	2.67	(0.19)	-0.45	(-2.78)	-1.35	(-0.61)
Max	-0.81	(-0.07)	-0.48	(-3.86)	-1.59	(-0.92)
Mom	-3.20	(-0.17)	-0.50	(-2.31)	-4.15	(-1.54)
Turn	5.59	(0.63)	-0.71	(-8.96)	-1.32	(-0.98)
Ztrade	5.58	(0.63)	-0.71	(-8.98)	-1.31	(-0.97)
$\beta_{\Delta \text{VIX}}$	2.01	(0.17)	-0.17	(-1.32)	-1.11	(-0.66)
Avg	0.91	(0.09)	-0.55	(-4.72)	-1.85	(-1.22)
Panel C: Commodities						
HML	2.84	(0.48)	-0.00	(-0.01)	-0.33	(-0.43)
Panel D: Options						
HML	-45.75	(-0.75)	-2.24	(-1.16)	-49.67	(-3.67)

Figure 5A shows that R^m has a U-shaped relationship with the contemporaneously realized monthly variance. The two black lines are regression lines fitted separately for the domain of positive and negative returns. It is evident that the relationship is not monotonically decreasing but has a stylized U-shape. Figure 5C shows that the same pattern is found for the realized pricing kernel implied by Equation (18).[15]

[15]The correlation between the realized M and the M^{VS} is 49%, indicating that the replication is far from perfect. However, to put this number into perspective, the correlation between the full pricing kernel and its projection in the equilibrium model in Section VI below is 30%. In addition, other factors

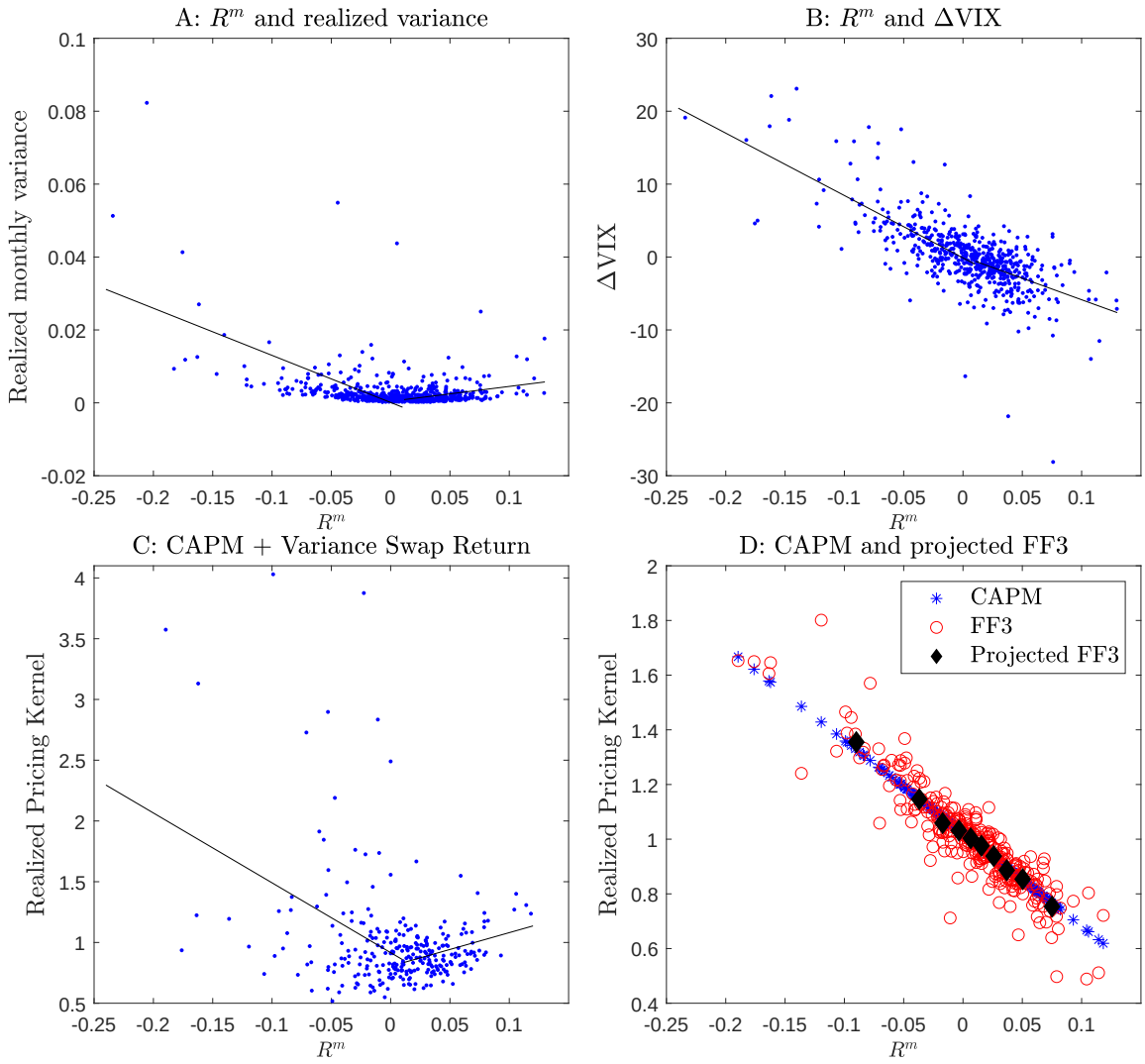

Figure 5: **Relationship between market return, factors, and pricing kernels.** Panel A shows the relationship between monthly market return R^m and contemporaneous realized monthly variance. Panel B shows the relationship between R^m and the contemporaneous change in the VIX index, ΔVIX. Panel C shows the realized pricing kernel for the CAPM + variance swap return model from Equation (19). Panel D shows the CAPM and the Fama-French three-factor (FF3) model projected onto market returns. The solid black lines are regression lines fitted in the domain of positive and negative returns separately. The projected FF3 pricing kernel is calculated by taking the average pricing in each decile of R^m.

Ang et al. (2006b) use a stock's beta with respect to daily changes in the VIX index ($\beta_{\Delta\text{VIX}}$) as their measure of a stock's exposure to changes in future expected variance. Figure 5B shows the relationship between R^m and the contemporaneous ΔVIX over the same time period.

might contribute to the replication error, such as noise in measurement, the pricing of variance risk being non-linear, or other risk premia being embedded in the option-implied M (e.g., jumps or higher moment risk).

Clearly, this relationship is monotonically decreasing. Furthermore, when considering that γ values of the $\beta_{\Delta\text{VIX}}$-sorted portfolios in Panel F of Table 1 are much lower than for all other sorts, these findings strongly suggest that a systematic variance risk factor based on $\beta_{\Delta\text{VIX}}$ captures neither curvature nor upside risk.

Taken together, the results from Figure 5 provide a possible explanation for why the $\beta_{\Delta\text{VIX}}$-factor in Ang et al. (2006b) cannot explain the Vol and Ivol anomaly, while my M and M^{VS} can. Lastly, the Figure 5D shows that the FF3 model projected onto index returns is also monotonically decreasing and, therefore, does not capture any upside risk premium.

VI. Upside Risk in an Equilibrium Model

This section derives the pricing implications of a long-run risks type model with recursive preferences where consumption growth and its variance feature GARCH-type dynamics. Due to the feedback process of high positive consumption shocks to variance, both large positive consumption shocks and large positive stock returns are associated with and increase in economic uncertainty. In equilibrium, the representative agent dislikes this increase in uncertainty more than she likes the associated positive consumption shock. Hence, these states are associated with high marginal utility, the projected M is U-shaped, and there is upside risk.

A. Setup

The model setup follows the long-run risks framework of Bansal and Yaron (2004). The representative agent has recursive Epstein and Zin (1989) preferences over total consumption. The dynamics of fundamentals are as follows:

$$x_{t+1} = \rho x_t + \rho_e \sigma_{c,t+1} \eta_{x,t+1} \tag{20}$$

$$g_{c,t+1} = \mu + x_t + \sigma_{c,t+1} \eta_{c,t+1} \tag{21}$$

$$g_{d,t+1} = \mu + \phi x_t + \pi \sigma_{c,t+1} \eta_{c,t+1} + \rho_d \sigma_{c,t+1} \eta_{d,t+1} \tag{22}$$

$$\sigma^2_{c,t+1} = w + b\sigma^2_{c,t} + a\sigma^2_{c,t}(\eta_{c,t} - h)^2 \tag{23}$$

$$\eta_{c,t+1}, \eta_{x,t+1}, \eta_{d,t+1} \sim i.i.d.\ N(0,1) \tag{24}$$

The dynamics of the long-run growth component x and log consumption growth g_c are identical to those in Bansal and Yaron (2004). Dividends are modeled with an exposure π to consumption shocks, which is absent in the original model but included in many follow-up specifications, such as Bansal et al. (2012) and Schorfheide et al. (2018). The key innovation is to replace the stochastic variance of the original model with the GARCH dynamics of Engle and Ng (1993), where the shocks to consumption growth have a feedback effect on future variance. This effect is symmetric around the parameter h; therefore, both large positive and large negative η_c leads to an increase in future σ^2_c (given the usual assumption of $w, a, b > 0$). This relationship is in contrast to the usual modeling frameworks of either pure stochastic variance or Markov chains,

where the shocks to g_c and σ_c^2 are assumed to be independent.

B. Estimation and evidence supporting GARCH dynamics

I estimate the GARCH dynamics with standard maximum likelihood.[16] The data are monthly real consumption growth per capita from 1959 to 2019. Panel A of Table 6 presents the estimation results, where statistical significance is based on a likelihood ratio test. All estimated parameters are highly significant, except h, which is significant at the 10% level. The implied long-run variance of 0.0041^2 is lower than the 0.0078^2 value used by Bansal and Yaron (2004). The estimated mean consumption growth parameter μ is relatively close to the sample mean of 0.00157, and the value in Bansal and Yaron (2004) of 0.0015. The implied persistence of σ_c^2 is 0.9966, which is higher than the 0.987 in Bansal and Yaron (2004) but lower than the 0.999 in Bansal et al. (2012).

The key property of the GARCH dynamics in the context of this paper is the quadratic, U-shaped effect of consumption shocks on future variance. To establish that both negative and positive shocks to consumption growth increase the future variance, I estimate the following alternative GARCH specification, which allows for different effects of positive and negative shocks:

$$\sigma_{c,t+1}^2 = w + b\sigma_{c,t}^2 + a\sigma_{c,t}^2(a^+\eta_{c,t}^2\mathbb{I}_{\eta_{c,t}>0} + a^-\eta_{c,t}^2\mathbb{I}_{\eta_{c,t}<0}^2). \tag{25}$$

The estimation results in Panel B of Table 6 show that both negative and positive shocks increase future variance. The estimated a^+ is even higher than the estimated a^-, which is in line with the estimated negative h in the benchmark specification.

C. Calibration

The estimated GARCH parameters imply a relatively high persistence of 0.9966, which leads to problems with the (numerical) solutions for some parameter combinations. I therefore slightly lower the estimated b parameter, such that the persistence is 0.992, which is between the 0.987 used in Bansal and Yaron (2004) and the 0.999 used in Bansal et al. (2012).[17] Furthermore,

[16] This possibility is another advantage over stochastic variance specifications, which require filtering techniques due to the latent nature of variance.

[17] In addition, I adjust w such that the average σ_c^2 remains unchanged. Changing the persistence does not affect the results qualitatively. I provide a detailed analysis and discussion of the sensitivity of the

Table 6: **Maximum Likelihood Estimates of GARCH Parameters.** The table shows the maximum likelihood parameter estimates for the GARCH dynamics specified in Equations (23) and (25). The data are monthly real consumption growth per capita from 1959 to 2019. p-values (in parentheses) are based on a likelihood ratio test.

LL	w	a	b	h	μ	a^+	a^-
Panel A: Benchmark							
3170.7	1.07×10^{-8} (0.000)	0.0298 (0.000)	0.964 (0.000)	-0.272 (0.083)	0.00137 (0.000)	-	-
Panel B: Monthly consumption growth and two a parameters							
3170.69	1.59×10^{-8} (0.000)	-	0.971 (0.000)	-	0.00138 (0.000)	0.0378 (0.000)	0.0184 (0.000)

I set $\pi = 2.6$ as in Bansal et al. (2012) and set $\phi = 1$. All other parameters are the same as in Bansal and Yaron (2004). Section IA.6 presents an analysis of the effect of changes in parameters on the main result.

D. Pricing implications

I solve the model numerically by iterating on the Euler equation, using a fine grid for the two state variables, x and σ_c^2.[18] For clarity, I denote the model's unprojected pricing kernel as M^{unproj} and the projection on the return on the aggregate dividend claim R^m, again, as M. In the model, M^{unproj} is given by

$$\ln(M_{t+1}^{unproj}) = \ln(\delta) - \gamma g_{c,t+1} - (\gamma - 1/\psi) \ln\left(\frac{V_{t+1}/C_{t+1}}{\mu_t(V_{t+1})/C_t}\right) \tag{26}$$

$$= \underbrace{\ln(\delta) - \gamma(\mu + x_t)}_{\text{constant}} \underbrace{-\gamma\sigma_{c,t+1}\eta_{c,t+1}}_{\text{linearly decreasing in } \eta_c} + \underbrace{(\gamma - 1/\psi)}_{>0} \underbrace{\ln\left(\frac{\mu_t(V_{t+1})/C_t}{V_{t+1}/C_{t+1}}\right)}_{\text{U-shaped in } \eta_c}, \tag{27}$$

where V_t is the continuation value of the investor's lifetime utility; $\mu_t(V_{t+1})$ is the certainty equivalent of the next period continuation value; γ is the coefficient of relative risk aversion; ψ is the elasticity of intertemporal substitution; and δ is the time discount factor. Figure 6A shows

main result with respect to all chosen parameters in IA.6.

[18] My solution builds on the code provided by Beason and Schreindorfer (2022), whom I thank for sharing.

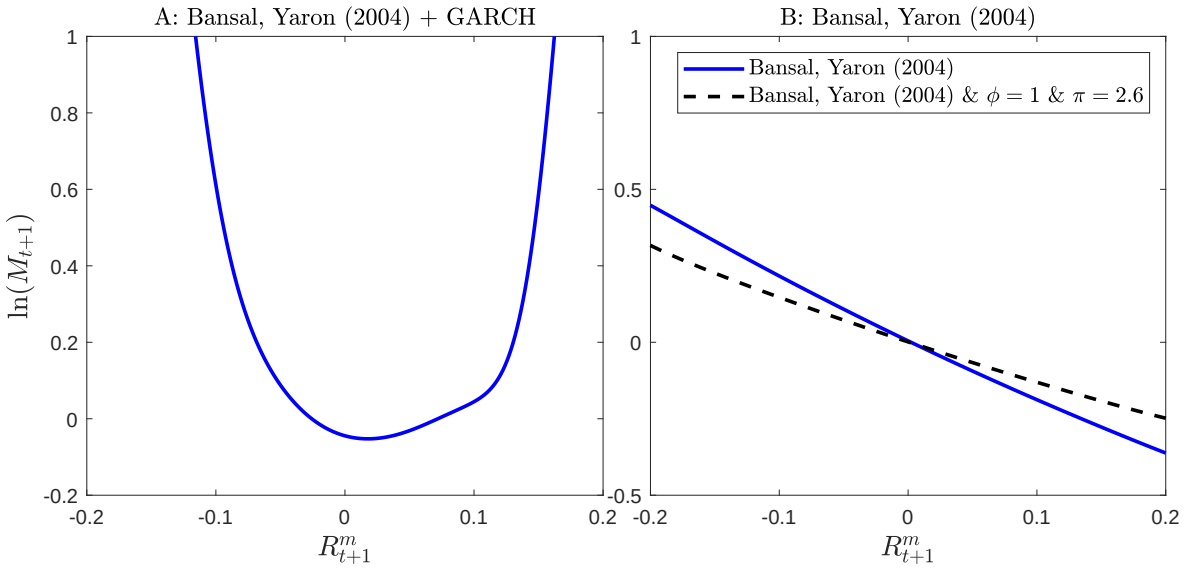

Figure 6: M **in the model.** This figure plots M, i.e., the pricing kernel projected on to market returns R^m, in the modified Bansal and Yaron (2004) model with GARCH dynamics in Panel A, and in the original model in Panel B. In Panel B, the blue line represents the original model, and the dashed black line represents a modified version that uses the same values for the parameters ϕ and π as the model with GARCH dynamics in this paper.

M, which is a U-shaped function of R^m. In contrast, in the original model, M is monotonically decreasing, as shown in Figure 6B. In short, the U-shape stems from large consumption growth shocks η_c leading to both high returns and high marginal utility.[19]

For a more detailed understanding of origins of the U-shaped M, I will next go through all relevant effects on M^{unproj} and R^m. First, note that the model has three shocks, but only η_c is important for the result because η_d is not priced and η_x affects returns positively and M^{unproj} negatively, i.e., leads to a strictly downward-sloping component in M. Hence, one only needs to understand the effects of η_c.

Next, consider the effect of η_c on M^{unproj}, which can partially be studied analytically as annotated in Equation (27). While the first term on the right-hand side is constant, the second term is the standard consumption shock term that implies that $\ln(M^{unproj})$ decreases linearly in η_c. The third term implies a U-shaped relationship between η_c and M^{unproj}, which can only be seen from the numerical solution. To understand the properties of the third term, one

[19]Technically, M depends on the two state variables x_t and $\sigma_{c,t+1}$ (which is known at time t). For ease of exposition, I fix x_t and $\sigma_{c,t+1}$ at their median for the graphs. However, all studied relationships are qualitatively unchanged for other $\sigma_{c,t+1}$ values, and for other x_t values they are even quantitatively the same (see IA.6 for details).

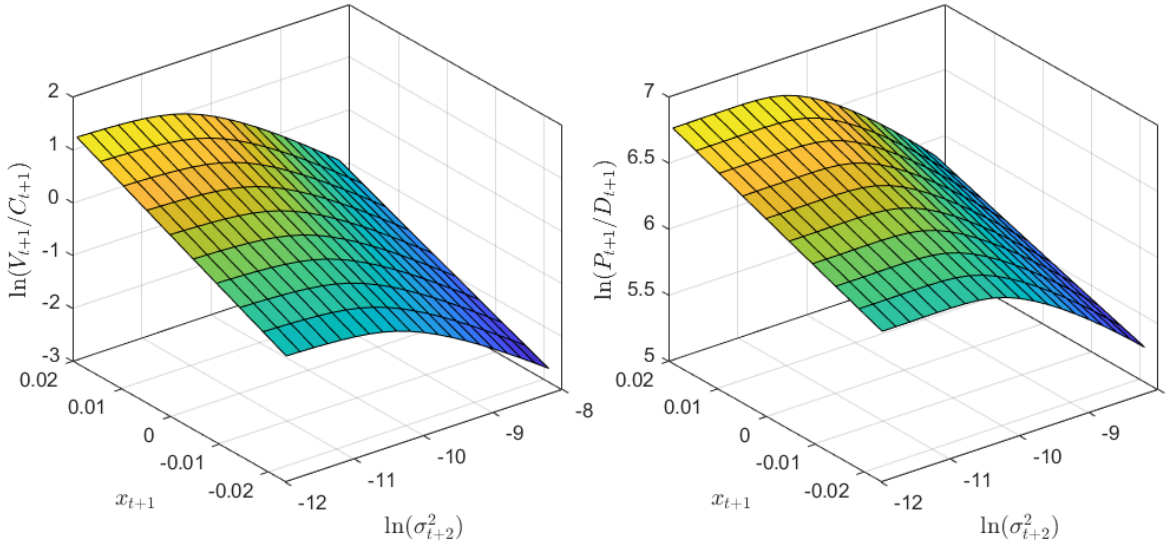

Figure 7: **Utility level and price-dividend ratio in the model.** The figure plots the natural logarithm of the ratio of utility level to consumption, $\ln(V_{t+1}/C_{t+1})$, and the natural logarithm of the price-dividend ratio, $\ln(P_{t+1}/D_{t+1})$, in the solved model against the two state variables.

needs to analyze the relationship between η_c and V/C. The left plot in Figure 7 shows that in equilibrium the V_{t+1}/C_{t+1} ratio is decreasing in $\sigma^2_{c,t+2}$ (which is known at time $t+1$), consistent with the original model.

In addition, recall that the variance dynamics imply that shocks to σ^2_c have a U-shaped relationship to η_c. Hence, the future V_{t+1}/C_{t+1} is inversely U-shaped in η_c, and the third term in Equation (27) is U-shaped in $\eta_{c,t+1}$. For negative η_c, all effects work in the same direction. For positive η_c, the increasing part of the U-shaped effect from the third term dominates the decreasing linear second term; consequently, the overall relationship between η_c and M^{unproj} is U-shaped, as depicted in the left plot of Figure 8.

Next, turning to returns, consider the effect of η_c on R^m. Note that

$$\ln(R^m_{t+1}) = g_{d,t+1} + \ln\left(\frac{P_{t+1}/D_{t+1}+1}{P_t/D_t}\right) \tag{28}$$

$$= \underbrace{\mu + \phi x_t}_{\text{constant}} + \underbrace{\rho_d \sigma_{c,t+1}\eta_{d,t+1}}_{\text{uncorrelated with } \eta_c} + \underbrace{\underbrace{\pi\sigma_{c,t+1}\eta_{c,t+1}}_{\text{linearly increasing in } \eta_c} + \underbrace{\ln\left(\frac{P_{t+1}/D_{t+1}+1}{P_t/D_t}\right)}_{\text{ambiguous in } \eta_c}}_{\text{“largely increasing in” } \eta_c}, \tag{29}$$

where the third term implies a linearly increasing relationship, and the fourth term is only

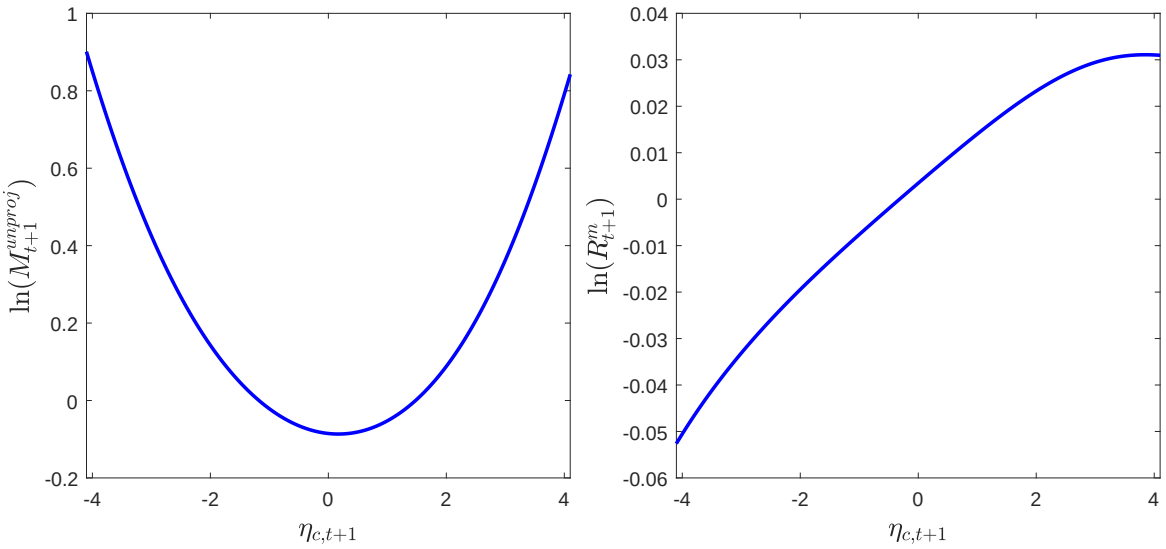

Figure 8: **Relationship between consumption shocks, pricing kernel and returns.** This figure plots the relationship between consumption growth shocks η_c and the average realized M^{unproj} in the left plot, and the relationship between η_c and the realized market return R^m in the right plot.

available numerically. The aggregate relationship between η_c and R^m is depicted in the right plot of Figure 8. For most of the (relevant) range of values of η_c, the relationship is monotonically increasing.

Taking all effects together, a high positive consumption shock η_c, on average, leads to a positive R^m due to a high positive dividend growth but also to an increase in σ_c^2, and hence a high realized M^{unproj}, which generates the U-shaped M depicted in Figure 6. In other words, a high positive R^m is, on average, associated with an increase in economic uncertainty, which the agent dislikes more than she likes the positive consumption growth associated with it. Hence, she wants to hedge against these states of the world, and assets that pay off well in these states (positive curvature relative to R^m) will have low average returns and negative CAPM alphas, and vice versa. Another way to illustrate these effects is that the model generates a one-period variance risk premium, while the original Bansal and Yaron (2004) model does not (not tabulated). This variance risk premium is a reflection of the fact that the agent is averse to large price movements, which is consistent with the empirical results above.

VII. Conclusion

This paper provides a novel approach to understanding several prominent stock return anomalies by using a pricing model extracted from options prices. The results show that a non-linear market model can jointly explain cross-sectional stock return anomalies related to beta, (idiosyncratic) volatility, liquidity, and momentum. A key part of the explanation is a new, negative upside risk premium, which is estimated to be 4.0% p.a., or on average almost half of the CAPM alphas of the anomalies. The same results are documented for European stock returns. Moreover, upside risk is also prevalent in other asset classes, such as options and commodities.

The paper further documents that many cross-sectional stock return anomalies have a negative relation between their CAPM alpha and the curvature of their returns relative to the market. This pattern is found for virtually all anomalies when the sorting is done based on return-based characteristics. Qualitatively, this pattern resembles the return profile of a short straddle, and hence the large positive alphas on straddles and stock returns anomalies are consistent. In contrast, anomalies based on accounting data have no noticeable curvature patterns.

The paper further provides a structural model that generates upside risk as a result of the positive correlation between shocks to economic fundamentals and an increase in economic uncertainty, and it provides supporting evidence for the main mechanism of the model. Empirically, the paper shows that the CAPM augmented by a second variance factor can also explain the studied anomalies. After controlling for the two factors, the strategies have only insignificant alphas left.

Appendix

A. Details on the Pricing Kernel Estimation

A.1. Options data

The empirical analysis uses out-of-the-money S&P 500 call and put options that are traded in the period from January 02, 1996 to December 31, 2019. I focus on the most liquid contract, namely, the standard third Friday contract (with AM settlement), to obtain a series of monthly pricing kernels with a 30-day horizon. Next, only options with positive trading volume are considered, and the standard filters proposed by Bakshi et al. (1997) are applied. I further clean the options data following the standard two-step approach in the literature:

1. For each month, find the third Friday option series that has a remaining time to maturity closest to 30 days. This step follows the standard approach in the literature to use data from Wednesdays, if available.
2. Remove all quotes that either have zero trading volume on the day of the price quote, have best bid below 0.50, are more than 20 index points in-the-money, or violate the standard no-arbitrage bounds considered by Bakshi et al. (1997).

Table A.1 presents descriptive statistics for the cleaned options data by standardized moneyness, i.e., $\tilde{K} = \ln(K/S_t)/\sigma_t$. The implied volatility (IV) mildly shows the typical volatility smirk pattern. The volume and open interest data show that the options contracts are highly liquid and traded for a large range of moneyness levels.

A.2. Estimation of the risk-neutral density

I use the following steps to estimate the risk-neutral density from options prices:

1. Clean the data as described above.
2. Get risk-free rates from OptionMetrics, and interpolate linearly for the correct maturity.
3. Get the dividend yield data from OptionMetrics and interpolate linearly for the correct maturity (using the implied dividend yield from at the money call and put pair leads to similar results, but the dividend yield estimates are more noisy).

Table A.1: **Options Data Descriptive Statistics**

The table presents descriptive statistics for the cleaned S&P 500 options data. The details of the data filters are given in Appendix A.1. The first column shows the total number of contracts over the sample period. The second column shows the average implied volatility (IV) in the percentage per annum (% p.a.). The third column shows the average volume per contract, and the last column shows the average open interest per contract. The data are all 30-day-to-maturity, out-of-the money, and third-Friday AM settled options contracts from January 02, 1996 to December 31, 2019.

$\tilde{K} = \frac{\ln(K/S_0)}{\sigma_t}$	Contracts	IV (% p.a.)	Volume	Open Interest
$\tilde{K} < -4$	4,860	32.1	1,561	9,712
$-4 < \tilde{K} < -3$	1,861	27.3	2,304	14,466
$-3 < \tilde{K} < -2$	2,123	24.7	2,533	16,756
$-2 < \tilde{K} < -1$	2,328	22.2	3,011	18,658
$-1 < \tilde{K} < 0$	3,594	18.6	3,684	17,953
$0 < \tilde{K} < 1$	3,687	16.0	3,229	15,971
$1 < \tilde{K} < 2$	2,250	14.4	2,119	14,703
$2 < \tilde{K}$	358	15.9	1,231	9,820

4. Transform mid-prices into implied volatilities using Black and Scholes (1973). In the region of +/- 20 points from at-the-money, take a weighted average (by volume) of put and call implied volatilities. The results remain unaltered if the implied volatility provided by OptionMetrics is used.

5. Fit a fourth-order polynomial to the implied volatilities over a dense set of strike prices, and convert back into call option prices using Black-Scholes.

6. Finally, numerically differentiate the call prices using Equations (30) and (31) to recover the risk-neutral return distribution:

$$1 - F^*(S_{t,t+\tau}) = -\exp(r\tau)\Big[\frac{\partial C_{BS}(S_t, X, \tau, r, \hat{\sigma}(S_t, X))}{\partial X}\Big]_{|X=S_{t,t+\tau}} \tag{30}$$

$$f^*(S_{t,t+\tau}) = \exp(r\tau)\Big[\frac{\partial^2 C_{BS}(S_t, X, \tau, r, \hat{\sigma}(S_t, X))}{\partial X^2}\Big]_{|X=S_{t,t+\tau}} \tag{31}$$

A.3. Estimation of the physical return density

The represented approach for obtaining the conditional physical density $f(R_{t+1})$ is semi-parametric and the most common methodology used in the literature to estimate the pricing kernel (see, e.g., Rosenberg and Engle (2002), Barone-Adesi et al. (2008), Christoffersen et al. (2013), Faias and

Santa-Clara (2017), or Christoffersen et al. (2022)). This method, often referred to as "filtered historical innovations," has several advantages. First and foremost, it is only semi-parametric as it only requires a minimum of parametric assumptions, preserves the empirical patterns for moments higher than two and, has a good fit to the empirical distribution. Moreover, the only parametric input is a forecast of conditional volatility (details in Appendix B), which can easily come from alternative models. Thus, the robustness analysis is straightforward.

The starting point is a long daily time series of the natural logarithm of monthly returns on the S&P 500 from January 02, 1990 to December 31, 2019, obtained from CRSP. The monthly return series is then standardized by subtracting the sample mean return $\bar{R}$ and then dividing by the conditional one-month volatility σ_t. This step yields a series of monthly return shocks Z:

$$Z_{t+1} = (R_{t+1} - \bar{R})/\sigma_t. \tag{32}$$

The conditional distribution f_{t+1} is then constructed by multiplying the standardized return shock series Z by the conditional monthly volatility expectation σ_t:

$$f_t(R_{+1}) = f\left(\bar{R} + \sigma_t Z\right). \tag{33}$$

In this paper, $f_t(R_{t+1})$ is calculated using only index return data available up to date t, i.e., f is obtained fully out-of-sample. To find a trade-off between using more recent and potentially more relevant data, on the one hand, and having as much data as possible for less noise in f, on the other hand, I use a rolling window of the past 10 years of return data as a compromise. The results are, however, fully robust to using a different window length or an expanding window.

B. Realized Variance Modeling

B.1. Overview

The goal is to forecast monthly (21 trading days) volatility. Bekaert and Hoerova (2014) conduct a large-scale, out-of-sample performance comparison of numerous state-of-the art heterogeneous autoregressive (HAR) realized variances models for the S&P 500 at the one-month horizon. They find that two specifications perform best: the HAR model combined with either the VIX

index or jumps as additional predictors. Building on these results, I focus on these predictors. For completeness, I also include the leverage effect considered in Bekaert and Hoerova (2014), and I confirm their finding that it is the least important predictor. In addition, I employ two recent advances from the literature that improve model performance. First, Bollerslev et al. (2016) show both theoretically and empirically that including realized quarticity corrects for measurement error in realized variance. Second, Clements and Preve (2021) show that estimating the model with weighted-least squares (WLS) instead of ordinary least squares (OLS) further improves out-of-sample forecasts.

The following section briefly lays out the econometric framework, followed by the empirical results. A more detailed discussion of each variable and its foundation in the literature can, for example, be found in Bekaert and Hoerova (2014).

B.2. Econometric framework

In the following, daily realized variance $RV_t^{(1)}$ is defined as the sum of N squared five-minute log returns $r_{t,i}$ of day t:

$$RV_t^{(1)} = \sum_{i=1}^{N} r_{t,i}^2. \tag{34}$$

Weekly ($h = 5$) and monthly ($h = 21$) RV is calculated as $RV_t^{(h)} = \frac{1}{h}\sum_{j=0}^{h-1} RV_{t-j}^{(1)}$. The daily jump $J_t^{(1)}$ is defined as

$$J_t^{(1)} = \max(RV_t - BV_t^{(1)} \cdot \pi/2, 0), \tag{35}$$

where $BV_t^{(1)}$ denotes the daily bipower variation:

$$BV_t^{(1)} = \sum_{i=1}^{N-1} |r_{t,i}||r_{t,i+1}|. \tag{36}$$

Jumps for other frequencies are calculated as $J_t^{(h)} = \frac{1}{h}\sum_{j=0}^{h-1} J_{t-j}^{(1)}$. The leverage effect at different frequencies is defined as $r_t^{(h)-} = \min\left(r_t^{(h)}, 0\right)$, where $r_t^{(h)} = \frac{1}{h}\sum_{j=0}^{h-1} r_{t-j}$. Lastly, following Bollerslev et al. (2016), daily realized quarticity $RQ_t^{(1)}$ is defined as

$$RQ_t^{(1)} = \frac{N}{3}\sum_{i=1}^{N} r_{t,i}^4, \tag{37}$$

and its multi-period analogue as $RQ_t^{(h)} = \frac{1}{h}\sum_{j=0}^{h-1} RQ_{t-j}^{(1)}$.

Taking all variables together, the most general model specification considered in the following (as well as in Bekaert and Hoerova 2014) is

$$\begin{aligned} RV_{t+21}^{(21)} =& c + \alpha VIX_t^2 + \underbrace{(\beta_d + \beta_{d,Q}(RQ_t^{(1)})^{1/2})}_{\beta_{d,t}} RV_t^{(1)} \\ &+ \underbrace{(\beta_w + \beta_{w,Q}(RQ_t^{(5)})^{1/2})}_{\beta_{w,t}} RV_t^{(5)} + \underbrace{(\beta_m + \beta_{m,Q}(RQ_t^{(21)})^{1/2})}_{\beta_{m,t}} RV_t^{(21)} \\ &+ \gamma_d J_t^{(1)} + \gamma_w J_t^{(5)} + \gamma_m J_t^{(21)} + \delta^d r_t^{(1)-} + \delta^w r_t^{(5)-} + \delta^m r_t^{(21)-} + \epsilon_{t+21}. \end{aligned} \tag{38}$$

Let $\widehat{RV_{t+21}^{(21)}}$ denote the out-of-sample forecast from the model estimated at day t using information available up to that day. The paper then refers to the expected variance over the next month, i.e., from day $t+1$ to $t+21$, as $\sigma_t^2 = \widehat{RV_{t+21}^{(21)}}$.

B.3. Model selection results

Next, I follow Bekaert and Hoerova (2014) and perform an out-of-sample model comparison of different model specifications. The keep the analysis simple and not to be overwhelmed by the large number of possible combinations of model specification and estimation method, I build on previous results showing that RV combined with jumps J and the VIX usually perform best. From this specification, I shut down either the VIX, J, or the RQ correction, or use OLS instead of WLS. Furthermore, motivated by the results in Bekaert and Hoerova (2014) that using single variables from a group of variables performs worse, all lags of one group of variables are included or excluded together. Lastly, I add the leverage effect to several model specifications.

The data are S&P 500 spot prices obtained from Tickdata.com as in Bekaert and Hoerova (2014) from January 02, 1990 to December 31, 2019. I use an initial burn-in period of six years, such that the first out-of-sample forecast is available at the beginning of 1996. I then extend the estimation window forward day by day.

To measure model performance, I follow Bekaert and Hoerova (2014) and use root mean squared error (RMSE), mean percentage error (MPE) and out-of-sample R^2 (R^2_{OOS}) as metrics.

Table A.2 presents the results. Overall, one can see that WLS always leads to large improvements over OLS, except for the specifications that include the leverage effect. Furthermore, the

specification without any adjustment to the estimation methodology (no RQ and OLS) has the worst accuracy.

I find that no model clearly outperforms in all metrics, which is analogous to Bekaert and Hoerova (2014). Therefore, I follow their approach and employ a ranking for each criterion, and calculate the average rank for each model in the last column of Table A.2. The ranking produces a clear winner: the model that includes both the VIX and jumps J via BV, estimated with WLS. This model ranks second in all metrics, while numerically being close to the best value for each metric, which is reflected in its overall best average rank. Therefore, I use this model as the benchmark model. The model with only the VIX is second best, with some distance to the next best one, which is the winning model estimated with OLS, tied with the model that only includes J. Similar to Bekaert and Hoerova (2014), I find that the leverage effect is the least important predictor variable. The full model including all variables performs worst (last two rows). Also, when adding the leverage effect to the second best model, the performance ranks low (above the last two rows).

Table A.2: **RV Model Statistics and Ranking**

The table shows statistics of the out-of-sample volatility forecasting model performance. Parameters are estimated using data from January 02, 1990 to December 31, 2019 using an extending window. Out-of-sample forecasts start on Jan 02, 1996. The first three columns show out-of-sample RMSE, MPE, and R^2_{OOS}. The next three column show the rank of each model for each criterion. The last column averages over the ranks. Bold font indicates the best value for each criterion.

Model	Method	RMSE	MPE	R^2_{OOS}	Rank	Rank	Rank	$\overline{\text{Rank}}$
VIX	OLS	0.0123	0.500	0.335	6	9	7	7.33
VIX	WLS	0.0093	0.466	**0.368**	3	4	1	2.67
J	OLS	0.0130	0.457	0.341	10	3	3	5.33
J	WLS	**0.0068**	0.470	0.292	1	5	10	5.33
VIX, J	OLS	0.0130	**0.452**	0.336	9	1	6	5.33
VIX, J	WLS	0.0085	0.455	0.366	2	2	2	**2.00**
VIX, J, no RQ	OLS	0.0127	0.502	0.281	8	10	12	10.00
VIX, J, no RQ	WLS	0.0104	0.472	0.316	4	6	9	6.33
VIX, r^-	OLS	0.0131	0.483	0.341	11	7	4	7.33
VIX, r^-	WLS	0.0118	0.559	0.340	5	12	5	7.33
VIX, J, r^-	OLS	0.0126	0.503	0.323	7	11	8	8.67
VIX, J, r^-	WLS	0.0136	0.493	0.291	12	8	11	10.33

C. Pricing Kernel Calculation

C.1. Anchoring the Pricing Kernel

It is necessary to "anchor" (adjust) M for the pricing analysis; otherwise, $E(M^{mon}) < 1/R_f$, i.e., it is not a valid pricing kernel. Therefore, the raw, unadjusted pricing kernel $\tilde{M}$ is anchored such that it prices the CRSP value-weighted market index (R^I in the following) correctly. The corrected M is obtained from adding a constant a to $\tilde{M}$, i.e.,

$$M = \tilde{M} + a, \tag{39}$$

where

$$a = 1 - \frac{1}{T}\sum_{t=1}^{T}\left(\tilde{M}_{t+1}R^I_{t+1}\right). \tag{40}$$

For the benchmark M, the value of a for the CAPM and the FF3 model is negligible, but for M^{mon}, the value of a is around 0.05.

For some of the robustness checks, the ratio of densities in Equation (13) becomes explosive in the tails. I therefore impose a maximum on the realized M of 4.53, which corresponds to the highest realized M of the benchmark method. This value is still large compared to the highest realized pricing kernels in the CAPM and FF3 model of 1.67 and 1.80, respectively.

C.2. Pricing kernel in linear factor models

One can represent the pricing kernel in a linear factor model as (see, e.g.,Cochrane (2005))

$$M_t = \bar{M} - bf_t, \tag{41}$$

where

$$b = E(f_t f_t')^{-1}\lambda \tag{42}$$

and λ denotes the market price of risk for each factor. For the CAPM, I use the CRSP value-weighted index, and λ is calculated using the sample mean of excess returns. Analogously, for the Fama-French three-factor model, I add the size and value factors obtained from Kenneth French's website.

D. Construction of Equity Portfolios

Following Bali et al. (2016), beta is estimated using a rolling window of one year of daily returns. Volatility (Vol) and idiosyncratic volatility (Ivol) are calculated over the most recent 21 trading days as in Ang et al. (2006b). The Max sort is based on the maximum daily return over the past 21 trading days as in Bali et al. (2011). Momentum (Mom) is the return over the past 12 months, excluding the last month as in Jegadeesh and Titman (1993). Turnover is calculated as number of shares traded as a fraction of the number of shares outstanding over the past year, as in Datar et al. (1998). The standardized turnover-adjusted number of zero daily trading volumes is calculated over the past year, as in Liu (2006). Beta with respect to changes in the VIX index ($\beta_{\Delta \text{VIX}}$) is calculated as in Ang et al. (2006a).

The 10 industry portfolios follow the classification provided by Kenneth French on his website. For the calculation of size, book-to-market (B/M), investment (Inv), and accruals (Acc), I follow the methodology used by Kenneth French.

Stock returns are obtained from CRSP, the risk-free rate and factors returns are from Kenneth French's website. Accounting data are from Compustat. I incorporate delisting returns based on the CRSP daily delisting file into the last return observation for the calculation of portfolio returns. Stocks are excluded if they have less then 180 valid return observations per year, or less than 12 observations for monthly variables. Lastly, stocks with a price below 1\$ (5\$ as robustness); an exchange code other than 1, 2, 3, or 31; or a share code other than 10 or 11 are excluded.

The SPX options expire at the market open ("AM") on the third Friday of each month. To accommodate this fact, I calculate "open returns" using the approach suggested by Polk et al. (2019). Specifically, for each stock, I divide the closing return on the settlement day by the intraday return of that day (open to close). The results remain qualitatively unchanged if the closing returns either from the expiry date or the preceding day are used. For commodities and European stock returns (ESTX options expire at 12:00) only closing prices exist, but the previous robustness check shows that this is a good approximation.

References

Aït-Sahalia, Y. and Lo, A. W. (2000), 'Nonparametric risk management and implied risk aversion', *Journal of Econometrics* **94**(1), 9–51.

Ang, A., Chen, J. and Xing, Y. (2006a), 'Downside risk', *Review of Financial Studies* **19**(4), 1191–1239.

Ang, A., Hodrick, R. J., Xing, Y. and Zhang, X. (2006b), 'The cross-section of volatility and expected returns', *Journal of Finance* **61**(1), 259–299.

Azzalini, A. and Capitanio, A. (2003), 'Distributions generated by perturbation of symmetry with emphasis on a multivariate skew t-distribution', *Journal of the Royal Statistical Society: Series B (Statistical Methodology)* **65**(2), 367–389.

Bakshi, G., Cao, C. and Chen, Z. (1997), 'Empirical performance of alternative option pricing models', *Journal of Finance* **52**(5), 2003–2049.

Bakshi, G., Crosby, J. and Gao Bakshi, X. (2022), 'Dark matter in (volatility and) equity option risk premiums', *Operations Research* **70**(6), 3035–3628.

Bakshi, G., Madan, D. and Panayotov, G. (2010), 'Returns of claims on the upside and the viability of u-shaped pricing kernels', *Journal of Financial Economics* **97**(1), 130–154.

Bali, T. G., Cakici, N. and Whitelaw, R. F. (2011), 'Maxing out: Stocks as lotteries and the cross-section of expected returns', *Journal of Financial Economics* **99**(2), 427–446.

Bali, T. G., Engle, R. F. and Murray, S. (2016), *Empirical asset pricing: The cross section of stock returns*, John Wiley & Sons.

Bansal, R., Kiku, D., Shaliastovich, I. and Yaron, A. (2014), 'Volatility, the macroeconomy, and asset prices', *Journal of Finance* **69**(6), 2471–2511.

Bansal, R., Kiku, D. and Yaron, A. (2012), 'An empirical evaluation of the long-run risks model for asset prices', *Critical Finance Review* **1**(1), 183–221.

Bansal, R. and Yaron, A. (2004), 'Risks for the long run: A potential resolution of asset pricing puzzles', *Journal of Finance* **59**(4), 1481–1509.

Banz, R. W. and Miller, M. H. (1978), 'Prices for state-contingent claims: Some estimates and applications', *Journal of Business* **51**(4), 653–672.

Barahona, R., Driessen, J. and Frehen, R. (2021), 'Can unpredictable risk exposure be priced?', *Journal of Financial Economics* **139**(2), 522–544.

Barberis, N. and Huang, M. (2008), 'Stocks as lotteries: The implications of probability weighting for security prices', *American Economic Review* **98**(5), 2066–2100.

Barone-Adesi, G., Engle, R. F. and Mancini, L. (2008), 'A garch option pricing model with filtered historical simulation', *Review of Financial Studies* **21**(3), 1223–1258.

Beason, T. and Schreindorfer, D. (2022), 'Dissecting the equity premium', *Journal of Political Economy* **130**(8), 2203–2222.

Bekaert, G. and Hoerova, M. (2014), 'The vix, the variance premium and stock market volatility', *Journal of Econometrics* **183**(2), 181–192.

Boguth, O., Carlson, M., Fisher, A. and Simutin, M. (2011), 'Conditional risk and performance evaluation: Volatility timing, overconditioning, and new estimates of momentum alphas', *Journal of Financial Economics* **102**(2), 363–389.

Bollen, N. P. and Whaley, R. E. (2004), 'Does net buying pressure affect the shape of implied volatility functions?', *Journal of Finance* **59**(2), 711–753.

Bollerslev, T., Patton, A. J. and Quaedvlieg, R. (2016), 'Exploiting the errors: A simple approach for improved volatility forecasting', *Journal of Econometrics* **192**(1), 1–18.

Breeden, D. T. and Litzenberger, R. H. (1978), 'Prices of state-contingent claims implicit in option prices', *Journal of Business* **51**(4), 621–651.

Broadie, M., Chernov, M. and Johannes, M. (2009), 'Understanding index option returns', *Review of Financial Studies* **22**(11), 4493–4529.

Brunnermeier, M. K., Gollier, C. and Parker, J. A. (2007), 'Optimal beliefs, asset prices, and the preference for skewed returns', *American Economic Review* **97**(2), 159–165.

Burnside, C. (2011), 'The cross section of foreign currency risk premia and consumption growth risk: Comment', *American Economic Review* **101**(7), 3456–76.

Campbell, J. Y., Giglio, S., Polk, C. and Turley, R. (2018), 'An intertemporal capm with stochastic volatility', *Journal of Financial Economics* **128**(2), 207–233.

Chabi-Yo, F. (2012), 'Pricing kernels with stochastic skewness and volatility risk', *Management Science* **58**(3), 624–640.

Chabi-Yo, F., Ruenzi, S. and Weigert, F. (2018), 'Crash sensitivity and the cross section of expected stock returns', *Journal of Financial and Quantitative Analysis* **53**(3), 1059–1100.

Cheng, I.-H. (2019), 'The vix premium', *Review of Financial Studies* **32**(1), 180–227.

Christoffersen, P., Heston, S. and Jacobs, K. (2013), 'Capturing option anomalies with a variance-dependent pricing kernel', *Review of Financial Studies* **26**(8), 1963–2006.

Christoffersen, P., Jacobs, K. and Pan, X. (2022), 'The state price density implied by crude oil futures and option prices', *Review of Financial Studies* **35**(2), 1064–1103.

Clements, A. and Preve, D. P. (2021), 'A practical guide to harnessing the har volatility model', *Journal of Banking & Finance* **133**, 106285.

Cochrane, J. H. (2005), *Asset pricing: Revised edition*, Princeton University Press.

Dahlquist, M. and Söderlind, P. (1999), 'Evaluating portfolio performance with stochastic discount factors', *Journal of Business* **72**(3), 347–383.

Datar, V. T., Naik, N. Y. and Radcliffe, R. (1998), 'Liquidity and stock returns: An alternative test', *Journal of Financial Markets* **1**(2), 203–219.

Dew-Becker, I. and Giglio, S. (2022), 'Risk preferences implied by synthetic options', *Working Paper* .

Dittmar, R. F. (2002), 'Nonlinear pricing kernels, kurtosis preference, and evidence from the cross section of equity returns', *Journal of Finance* **57**(1), 369–403.

Engle, R. F. and Ng, V. K. (1993), 'Measuring and testing the impact of news on volatility', *Journal of Finance* **48**(5), 1749–1778.

Epstein, L. G. and Zin, S. E. (1989), 'Substitution, risk aversion, and the temporal behavior of consumption and asset returns: A theoretical framework', *Econometrica* **57**(4), 937–969.

Faias, J. A. and Santa-Clara, P. (2017), 'Optimal option portfolio strategies: Deepening the puzzle of index option mispricing', *Journal of Financial and Quantitative Analysis* **52**(1), 277–303.

Fama, E. F. and French, K. R. (1993), 'Common risk factors in the returns on stocks and bonds', *Journal of Financial Economics* **33**(1), 3–56.

Farago, A. and Tédongap, R. (2018), 'Downside risks and the cross-section of asset returns', *Journal of Financial Economics* **129**(1), 69–86.

Figlewski, S. (2010), 'Estimating the implied risk neutral density for the us market portfolio', *Volatility and Time Series Econometrics: Essays in Honor of Robert Engle* pp. 323–353.

Frazzini, A. and Pedersen, L. H. (2022), 'Embedded leverage', *Review of Asset Pricing Studies* **12**(1), 1–52.

Garleanu, N., Pedersen, L. H. and Poteshman, A. M. (2008), 'Demand-based option pricing', *Review of Financial Studies* **22**(10), 4259–4299.

Gormsen, N. J. and Jensen, C. S. (2022), 'Higher-moment risk', *Available at SSRN 3069617* .

Gu, S., Kelly, B. and Xiu, D. (2020), 'Empirical asset pricing via machine learning', *Review of Financial Studies* **33**(5), 2223–2273.

Harvey, C. R. and Siddique, A. (2000), 'Conditional skewness in asset pricing tests', *Journal of Finance* **55**(3), 1263–1295.

Jackwerth, J. C. (2000), 'Recovering risk aversion from option prices and realized returns', *Review of Financial Studies* **13**(2), 433–451.

Jegadeesh, N. and Titman, S. (1993), 'Returns to buying winners and selling losers: Implications for stock market efficiency', *Journal of Finance* **48**(1), 65–91.

Kelly, B. and Jiang, H. (2014), 'Tail risk and asset prices', *Review of Financial Studies* **27**(10), 2841–2871.

Kraus, A. and Litzenberger, R. H. (1976), 'Skewness preference and the valuation of risk assets', *Journal of Finance* **31**(4), 1085–1100.

Lettau, M., Maggiori, M. and Weber, M. (2014), 'Conditional risk premia in currency markets and other asset classes', *Journal of Financial Economics* **114**(2), 197–225.

Liu, W. (2006), 'A liquidity-augmented capital asset pricing model', *Journal of Financial Economics* **82**(3), 631–671.

Mitton, T. and Vorkink, K. (2007), 'Equilibrium underdiversification and the preference for skewness', *Review of Financial Studies* **20**(4), 1255–1288.

Newey, W. K. and West, K. D. (1987), 'A simple, positive semi-definite, heteroskedasticity and autocorrelation consistent covariance matrix', *Econometrica* **55**(3), 703–708.

Parker, J. A. and Julliard, C. (2005), 'Consumption risk and the cross section of expected returns', *Journal of Political Economy* **113**(1), 185–222.

Polk, C., Lou, D., Skouras, S., Lou, D., Polk, C. and Skouras, S. (2019), 'A tug of war: Overnight versus intraday expected returns', *Journal of Financial Economics* **134**(1), 192–213.

Rosenberg, J. V. and Engle, R. F. (2002), 'Empirical pricing kernels', *Journal of Financial Economics* **64**(3), 341–372.

Schneider, P., Wagner, C. and Zechner, J. (2020), 'Low-risk anomalies?', *Journal of Finance* **75**(5), 2673–2718.

Schorfheide, F., Song, D. and Yaron, A. (2018), 'Identifying long-run risks: A bayesian mixed-frequency approach', *Econometrica* **86**(2), 617–654.

Sichert, T. (2023), 'The pricing kernel is u-shaped', *Available at SSRN 3095551* .

Song, Z. and Xiu, D. (2016), 'A tale of two option markets: Pricing kernels and volatility risk', *Journal of Econometrics* **190**(1), 176–196.

Tédongap, R. (2015), 'Consumption volatility and the cross-section of stock returns', *Review of Finance* **19**(1), 367–405.